

제 2 차 년 도
최 종 보 고 서

KIER - 966413

고급산화 수처리를 위한
high quantum yield 혼합광촉매 개발과
최적의 solar detoxification system 개발

Development of Mixed Oxide Photocatalysts and
Optimized Solar Detoxification System for the Treatment
of wastewater by Advanced Oxidation

연 구 기 관

한국에너지기술연구소

과 학 기 술 처

서 지 정 보 양 식		1. 보고서번호 KIER-966413
2. 서명 : 부서명 고급산화 수처리를 위한 high quantum yield 혼합광촉매 개발과 최적의 solar detoxification system 개발		
3. 보고서 종류: 최종보고서	4. 수행 부서명 태양에너지응용연구팀	
5. 연구수행자(연구책임자 맨앞에 기재) 이태규; 전명석; 주현규; 조덕기; 김홍제; 이순명; 전일수		
6. 보고서 발행일 1997. 9. .	7. 페이지(서문, 본문) xi, 77	8. 참고사항 도표(3)개/그림(33)개/참고문헌(20)개
9. 위탁기관 과학기술처	10. 공개여부 공개 (○) 비공개 (까지)	
11. 초록 (250단어 내외) <p>본 한국-독일 국제공동연구 사업의 최종적인 목표는 산업화된 전세계적인 문제인 수질오염 문제의 환경 친화적인 해결을 위한 혼합광촉매와 이를 이용한 처리시스템의 개발이다. 다시 말해서 광화학반응에서 자외선 영역의 광에너지 이용을 줄이고 보다 장파장의 영역을 이용하기위한 혼합광촉매의 제조가 주목적이라 할 수 있다. 또한 이 기술은 태양에너지 또는 전기에너지를 활용함으로써 지구의 온난화 및 화석연료의 고갈을 방지할 수 있으므로 지구의 환경오염을 방지 또는 개선할 수 있는 기술이다. 기존의 처리기술과 비교하여 시스템의 운전조건이 용이하고, 에너지 소모가 적으며, 2차처리 공정이 생략될 수 있어서 시스템의 구성 및 운전비용, 유지비용이 크게 절감될 수 있다.</p> <p>Sol-gel법을 비롯한 여러 방법으로 순수한 titanium dioxide (TiO₂)와 세 가지의 혼합광촉매 (Fe/Ti, Ni/Ti, Zn/Ti)를 제조하여 Actinometry, EDAX, UV/VIS, FTIR, TEM등을 이용하여 성질을 분석하였다. 또한 제조된 촉매를 이용하여 bench-scale과 옥외 반응 system을 이용하여 dichloroacetate (DCA)와 반도체 제조공장의 실패수 분해를 실시하였다. 제조된 혼합광촉매 중 Fe/Ti 촉매는 bandgap energy가 낮아졌음을 의미하는 UV/VIS absorbance의 red-shift를 나타내었다. 이외의 Ni/Ti와 Zn/Ti는 blue-shift를 보여주었다. 이는 FTIR결과에서 나타난 OH기의 Fe 함량의 다른 증가로 간접적인 뒷받침이 되었다</p>		
12. 주제코드 140505; 400500; 540300		
13. 키워드(10개 내외) 고급산화; 광촉매; 광화학반응; 폐수처리; 광효율		

BIBLIOGRAPHIC INFORMATION SHEET		1. REPORT NO. KIER-966413
2. TITLE : SUBTITLE Development of Mixed Oxide Photocatalysts and Optimized Solar Detoxification System for the Treatment of wastewater by Advanced Oxidation		
3. TYPE OF REPORT Final Report	4. PERFORMING LAB. Applied Solar Energy Research Team	
5. RESEARCHER T.K.Lee; M.S.Jeon; H.K.Joo; D.K.Jo; H.J.Kim; S.M.Lee; I.S.Jeon		
6. REPORT DATE 1997. 9. .	7. TOTAL PAGES xi, 77	8. REFERENCE Tabs.(3) / Figs.(33) / Refs.(20)
9. SPONSORING ORGANIZATION Ministry of Science & Technology	10. CLASSIFIED OPEN (<input checked="" type="radio"/>) NOT OPEN (<input type="radio"/>)	
11. ABSTRACT (About 250 words) <p>The primary purpose of this Korea-Germany joint research is the development of environmentally benign photocatalysts and detoxification system with these catalysts for the wastewater treatment over the world. In other words, development of mixed oxide photocatalysts, which can reduce the use of UV region but increase the part of visible region of wavelength, is a main target of this research. In this process, since sunlight or generated electric power is used as the energy source, it could prevent from the global warming and shortage of the fossil fuel, thus, improves the global environmental situation. The structural facilities and instrumentation with this system are relatively easy, and energy cost is minimal. Further more, this system does not require any secondary treatment for the process.</p> <p>In this project, three different mixed oxides such as Fe/Ti, Ni/Ti, and Zn/Ti as well as pure titanium oxide (TiO₂) were prepared by Sol-Gel method and others. These catalysts were analyzed by actinometry, EDAX, UV/VIS, FTIR, and TEM in terms of physical and chemical properties. With these mixed oxides, experiments using bench-scale and outside solar reaction system were performed to degrade real wastewater from a electronics company.</p> <p>Among mixed oxides Fe/Ti resulted in red-shifted UV/VIS absorbance, implying that bandgap energy of this mixed oxide is lower than pure titanium dioxide. Meanwhile, Ni/Ti and Zn/Ti showed the opposite trend in absorbance. This result was supported by FTIR analysis, which produced the increasing peak area for OH group as Fe content increased.</p>		
12. SUBJECT CATEGORY 140505; 400500; 540300		
13. KEYWORD advanced oxidation; photocatalyst; photocatalysis; wastewater; quantum yield; photonic efficiency		

요 약 문

I. 제 목

고급산화 수처리를 위한 high quantum yield 혼합광촉매 개발과 최적의 solar detoxification system 개발

II. 연구개발의 목적 및 중요성

본 한국-독일 국제공동연구 사업의 최종적인 목표는 산업화된 전세계적인 문제인 수질오염 문제의 환경 친화적인 해결을 위한 혼합광촉매와 이를 이용한 처리시스템의 개발이다. 다시 말해서 광화학반응에서 자외선 영역의 광에너지 이용을 줄이고 보다 장파장의 영역을 이용하기 위한 혼합광촉매의 제조가 주목적이라 할 수 있다. 또한 이 기술은 태양에너지 또는 전기에너지를 활용함으로써 지구의 온난화 및 화석연료의 고갈을 방지할 수 있으므로 지구의 환경오염을 방지 또는 개선할 수 있는 기술이다. 기존의 처리 기술과 비교하여 시스템의 운전조건이 용이하고, 에너지 소모가 적으며, 2차처리 공정이 생략될 수 있어서 시스템의 구성 및 운전비용, 유지비용이 크게 절감될 수 있다.

광화학반응 연구분야에서 우수연구 기관중의 하나인 독일의 Institut für

Solarenergie Forschung, GmbH 와의 공동연구는 그 연구결과를 실용화로 이끌어 지구환경 개선에 일익을 담당할 것이다. 이 공동연구를 통하여 시스템의 실용화가 달성되면 값비싼 해외 선진기술의 도입대신, 개발도상국 또는 제 3 국가에 기술 또는 시스템 수출도 추진할 수 있으리라 생각된다.

III. 연구개발의 내용 및 범위

Sol-gel 법을 비롯한 여러 방법으로 순수한 titanium dioxide (TiO_2)와 세 가지의 혼합광촉매 (Fe/Ti, Ni/Ti, Zn/Ti)를 제조하여 Actinometry, EDAX, UV/VIS, FTIR, TEM 등을 이용하여 성질을 분석하였다. 또한 제조된 촉매를 이용하여 bench-scale 과 옥외 반응 system 을 이용하여 dichloroacetate (DCA)와 반도체 제조공장의 실폐수 분해를 실시하였다.

IV. 연구결과 및 활용

- (1) EDAX 결과에서 보듯이 제조된 촉매는 이론상 의도된 양만큼의 성분을 포함하고 있어, 촉매들이 잘 제조되었음을 증명하였다.
- (2) 제조된 혼합광촉매 중 Fe/Ti 촉매는 bandgap energy 가 낮아졌음을 의미하는 UV/VIS absorbance 의 red-shift 를 나타내었다. 이외의 Ni/Ti 와 Zn/Ti 는 blue-shift 를 보여주었다. 이는 FTIR 결과에서 나타난 $-\text{OH}$ 기의 Fe

함량의 다른 증가로 간접적인 뒷받침이 되었다.

(3) Actinometry 를 위한 DCA 분해 효율에서도 Fe/Ti 가 다른 두 종류보다 월등히 우수하였다.

(4) 실험수 적용에서는 희석의 비가 (초기농도)가 중요한자로 작용되었다.

이와 같이 혼합광촉매를 이용한 실험수의 태양에너지를 이용한 처리 가능성과 system 의 제반조건을 확립하였다. 이러한 연구결과를 토대로 향후 산업 폐수 처리에 활용 가능한 광화학반응기 설계 및 제에 이용할 예정이다.

여 백

Summary

I. Title

Development of Mixed Oxide Photocatalysts and Optimized Solar Detoxification System for the Treatment of wastewater by Advanced Oxidation.

II. Purpose and Importance

The primary purpose of this Korea-Germany joint research is the development of environmentally benign photocatalysts and detoxification system with these catalysts for the wastewater treatment over the world. In other words, development of mixed oxide photocatalysts, which can reduce the use of UV region but increase the part of visible region of wavelength, is a main target of this research. In this process, since sunlight or generated electric power is used as the energy source, it could prevent from the global warming and shortage of the fossil fuel, thus, improves the global environmental situation. The structural facilities and instrumentation with this system are relatively easy, and energy cost is minimal. Further more, this system does not require any secondary treatment for the process.

The joint project with well-known institute like Institut für Solarenergie

forschung, GmbH (ISFH, Germany) can be mutually advantageous in improving world environment by commercialization. Besides, it is essential to accumulate the fundamental technologies and to establish the Korean system in order not to pay any royalty to the advanced countries. Actually the success of this project could bring a possibility to export this technique or system to the some underdeveloped countries.

III. Contents and Scope

In this project, three different mixed oxides such as Fe/Ti, Ni/Ti, and Zn/Ti as well as pure titanium oxide (TiO_2) were prepared by Sol-Gel method and others. These catalysts were analyzed by Actinometry, EDAX, UV/VIS, FTIR, and TEM in terms of physical and chemical properties. With these mixed oxides, experiments using bench-scale and outside solar reaction system were performed to degrade real wastewater from a electronics company.

IV. Results and Applications

(1) Like shown in EDAX analysis, the prepared mixed oxide was proven to have intended amount of impurity.

- (2) Among mixed oxides Fe/Ti resulted in red-shifted UV/VIS absorbance, implying that bandgap energy of this mixed oxide is lower than pure titanium dioxide. Meanwhile, Ni/Ti and Zn/Ti showed the opposite trend in absorbance. This result was supported by FTIR analysis, which produced the increasing peak area for –OH group as Fe content increased.
- (3) In Actinometry, DCA was degraded more by Fe/Ti than by others.
- (4) For real wastewater, optimum initial concentration was present (initial value of TOC and COD).

The possibility and design information of treating wastewater using mixed oxides were set like aforementioned. On the basis of results obtained in this project, photocatalytic system design for industrial wastewater will be proceeded.

여 백

Contents

Chapter 1. Background	1
Chapter 2. Review	4
2.1 Process description	
2.2 Photoactive semiconductors	
2.3 Photoreactors for solar application	
Chapter 3. Experimental	16
3.1 Synthesis of mixed oxide catalysts	
3.2 Measurement of photonic efficiency	
3.3 Fourier transformed infrared spectrometer analyses	
3.4 Double sheet skin photoreactor for real wastewater treatment	
Chapter 4. Results and Discussion	25
4.1 UV/VIS absorbance	
4.2 Actinometry	
4.3 DCA degradation and photonic efficiencies	
4.4 EDAX and FTIR	
4.5 Real wastewater treatment study	
Chapter 5. Conclusions	61
References	62
Appendix	65
Photograph images and photoreactor design	

List of Figures and Tables

Table 2.1	List of compounds that have been destroyed using photoassisted heterogeneous catalytic oxidation	5
Figure 2.1	Energy level band diagrams for three types of solids	7
Table 2.2	Summary of several semiconductors and their bandgap energies and wavelength of light energy equivalent to the bandgap	9
Figure 2.2	Relative electron potential of a photocatalyst and redox potential of an aqueous solution	10
Figure 2.3	Simplified schematic of the photoactivation mechanisms of an intrinsic semiconductor	11
Figure 3.1	Schematic diagram of rotary evaporator	17
Figure 3.2	Schematic diagram of reaction system	23
Table 3.1	Chemical data sheet of the wastewaters H ₂ O ₂ and ORG and the mixed water	24
Figure 4.1	UV/VIS Absorbancies of Fe/Ti samples while dialyzing	28
Figure 4.2	UV/VIS Absorbancies of Ni/Ti samples while dialyzing	29
Figure 4.3	UV/VIS Absorbancies of Zn/Ti samples while dialyzing	30
Figure 4.4	UV/VIS Absorbancies of Ni/Ti colloids	31
Figure 4.5	UV/VIS Absorbancies of Zn/Ti colloids	32
Figure 4.6	Amount of added NaOH for degradation of DCA with Ni/Ti	33
Figure 4.7	Amount of added NaOH for degradation of DCA with Zn/Ti	34
Figure 4.8	Comparison of photonic efficiency between Ni/Ti and Zn/Ti	35

Figure 4.9	Photonic efficiency for Fe/Ti	36
Figure 4.10	FTIR for Fe/Ti	38
Figure 4.11	FTIR for Ni/Ti	39
Figure 4.12	FTIR for Zn/Ti	40
Table 4.1	Emission limitations in Korea	41
Figure 4.13	H ₂ O ₂ /ORG (1:1), 1 g /1 P25, pH=9.3	47
Figure 4.14	H ₂ O ₂ /ORG (1:1), 5 g /1 P25, pH=8.8	48
Figure 4.15	H ₂ O ₂ /ORG (1:1), 5 g /1 Hombikat, pH=7.6	49
Figure 4.16	H ₂ O ₂ /ORG (1:1), 5 g /1 Hombikat, pH=7.6(II)	50
Figure 4.17	Lab experiment, H ₂ O ₂ , 1 g /1 P25, pH=3.O ₂ , UV-C	51
Figure 4.18	H ₂ O ₂ /ORG (1:1), 5 g /1 Hombikat, pH=2.9, air	52
Figure 4.19	ORG, 5 g /1 Hombikat, pH=2.9, air	53
Figure 4.20	ORG, 5 g /1 P25, pH=2.6, air	54
Figure 4.21	Efficiencies for H ₂ O ₂ /ORG without pH adjusting using different catalysts	55
Figure 4.22	Efficiencies for H ₂ O ₂ /ORG with 5 g /1 Hombikat and different pH	56
Figure 4.23	Efficiencies for ORG with pH adjusting using different catalysts	57
Figure 4.24	Influence of H ₂ O ₂ on efficiency with pH adjusting using 5 g /1 Hombikat	58

Chapter 1 Background

The increasingly clear need for new and effective methods for cleaning polluted air and water systems has recently resulted in a renewed interest in developing environmentally benign methods for detoxification, possibly by complete mineralization of a wide range of organic compounds. Even though biodegradation with microorganisms and chemical treatment with chlorine or ozone has been conventionally used for detoxification, they are limited by lethal effect of toxic compounds to microorganisms and incomplete purification and by the need for large quantities of the oxidizing reagent. For this reason the need for an alternative, environmentally benign method, for complete mineralization of various organic compounds has been initiated. Several methods, each of them being one of so called “advanced oxidation processes (AOPs)”, have been investigated by many researchers. These methods employ a high-energy source to induce chemical reduction/oxidation reactivity. They are affected by adsorption, pH of aqueous phase, surface heterogeneity, and others. Among several AOPs using ultraviolet light (UV) as an energy source, photocatalysis with suspended powder or immobilized form of semiconductor has attracted many investigators’ attention. Most frequently used semiconductor is titanium dioxide (TiO_2) because this satisfies the required conditions such as no toxicity, stability in aqueous solution, and no photocorrosion under band gap illumination. Titanium dioxide has bandgap energy (E_g) of 3.2 eV and thus, needs light below 380 nm to be capable of e^-/h^+ pairs. Because light below

400 nm of wavelength is only 5% of the solar energy reaching the surface of the earth, for solar applications novel catalysts have to be developed which have similar efficiencies as anatase TiO₂, but absorb in the visible part of the solar spectrum and simultaneously improve the photocatalytic detoxification properties in this spectral region. For this reason it was initiated to envisage mixed oxide which can exhibit a red-shifted absorption spectrum and also a suppressed recombination of charge carriers compared to pure TiO₂. Besides, quantum-size photocatalysts has recently been studied because this size semiconductor particle (critical radius of 10 nm) behaves quantum mechanically as a simple particle in a box, resulting in increased band gap energy (blue-shifted), enlarged redox potentials, and hindered e⁻/h⁺ recombination.

The environmental problems are not limited to any specific countries, but the whole world is suffering from or will be faced to such crises. Utilization of solar energy, which is free of charge and abundant, for improving environmental problems on earth was proposed by both Korea Institute of Energy Research (KIER), Korea and Institut für Solarenergieforschung, GmbH (ISFH), Germany in 1996. Both parties are agreed to share the knowledge and information on the solar detoxification processes with heterogeneous photocatalytic reaction. ISFH is well known as one of the main institutes for the utilization of solar energy in the world and has performed profound researches on the synthesis of novel photocatalysts and design of photoreactor. Meanwhile, KIER also has carried out solar detoxification for wastewater remediation with its own solar facilities in the presence of home-made photocatalysts. Besides the

institute has a great deal of experience in treating real wastewater by solar or artificial light source from various industries such as dyeing company, photo printing facility, paper-making factory, power generation company, etc. For some of them commercialization process is under way. Thus this joint project was undertaken mainly to synthesize high photonic efficiency mixed oxide photocatalysts and to optimize solar detoxification system through comparing both institutes for the early commercialization for wastewater treatment.

Chapter 2 Review

2.1 Process description

Photoassisted heterogeneous catalytic oxidation involves the use of photoactive n-type semiconductor powders and near-UV light. When these semiconductors are illuminated in water, a redox environment is established that can cause the oxidation of organic compounds. In most cases, the crystalline anatase form of titanium dioxide has been used as the semiconductor because of its high activity and stability. Laboratory studies (Hermann and Pichat 1980; Ollis et al. 1984; Pruden and Ollis 1983; Hsiao et al. 1983; Okamoto et al. 1985; Matthews 1987a, 1987b, 1988; Ohnishi et al. 1989; Al-Ekabi and Serpone 1988) have demonstrated that a wide variety of organic compounds, such as chlorinated alkanes and alkenes, polychlorinated phenols, aromatics, aldehydes, and organic acids, can be oxidized using near-UV or solar illuminated TiO₂ aqueous suspensions.

Table 2.1 lists many of the compounds that have been successfully destroyed using this process and many other compounds were also reported (Blake et al. 1996). Most were completely mineralized to such compounds as carbon dioxide, water, and hydrochloric acid. A number of the compounds listed in the table are important to the water industry because they are DBPs. However, studies have shown that some nitrogen-containing compounds, such as atrazine, are difficult to mineralize with this

process. For example, Pelizzetti et al.(1990) reported that atrazine was photocatalytically oxidized to cyanuric acid.

Table 2.1 List of compounds that have been destroyed using photoassisted heterogeneous catalytic oxidation

phenol	chloroform	4-chlorophenol
trichloroethene	2-chlorophenol	1,2-dichloroethane
salicylic acid	1,2-dibromomethane	benzoic acid
dichloromethane	biphthalates	carbon tetrachloride
chlorobenzene	chloromethane	nitrobenzene
dichloroacetaldehyde	methanol	tetrachloroethene
ethanol	dichloroacetic acid	n-propanol
monochloroacetic acid	2-propanol	1,1,1-trichloroethane
acetone	2,4-dichlorophenol	ethyl acetate
2,4,5-trichlorophenol	acetic acid	o-dichlorobenzene
formic acid	p-dichlorobenzene	sucrose
bromoform	2-naphtol	difluorodichloromethane
umbelliferone	vinyl bromide	hydrogen sulfide
lignin	cyanide	

At the present time, development of photoassisted heterogeneous catalytic oxidation for destroying organic contaminants is at the pilot-scale stage, and several pollution equipment companies and research laboratories are moving toward its commercialization. For example, one company in USA recently received funding from the USEPA for a pilot-plant demonstration of its photoassisted heterogeneous catalytic oxidation system. In the process developed by this company, TiO_2 is coated onto a fiberglass mesh, which is wrapped around near-UV lamps and placed in a stainless-steel reactor. The contaminated water is then pumped through the jacket so that it comes in contact with the illuminated TiO_2 and the contaminants are oxidized. In another process, developed and pilot tested by researchers from Sandia National Laboratories, a linear parabolic sun tracking solar collector concentrates sunlight onto a UV-transmitting reactor containing TiO_2 powder suspended in contaminated water. The reactor is capable of mineralizing 5 ppm of trichloroethane to 5 ppb in about 4 min at a rate of 42 L/min.

The photoassisted heterogeneous catalytic oxidation process is an emerging water and waste treatment technology. However, major engineering strides must be taken if this process is to become viable and cost effective.

2.2 Photoactive semiconductors

Solids, or crystalline minerals, are categorized as conductors, semiconductors, or insulators according to their ability to conduct electrical current. Figure 2.1 consists

of the electron energy level diagrams for conductors, insulators, and semiconductors. The valence band (VB) is the energy level occupied by the outermost electrons in a solid. The conduction band (CB) is the highest energy level in an atom. Because it is unoccupied by electrons at the ground state, electrons from the VB can move into it and are free to flow within the solid. The VB and CB are often separated by an energy barrier called the bandgap.

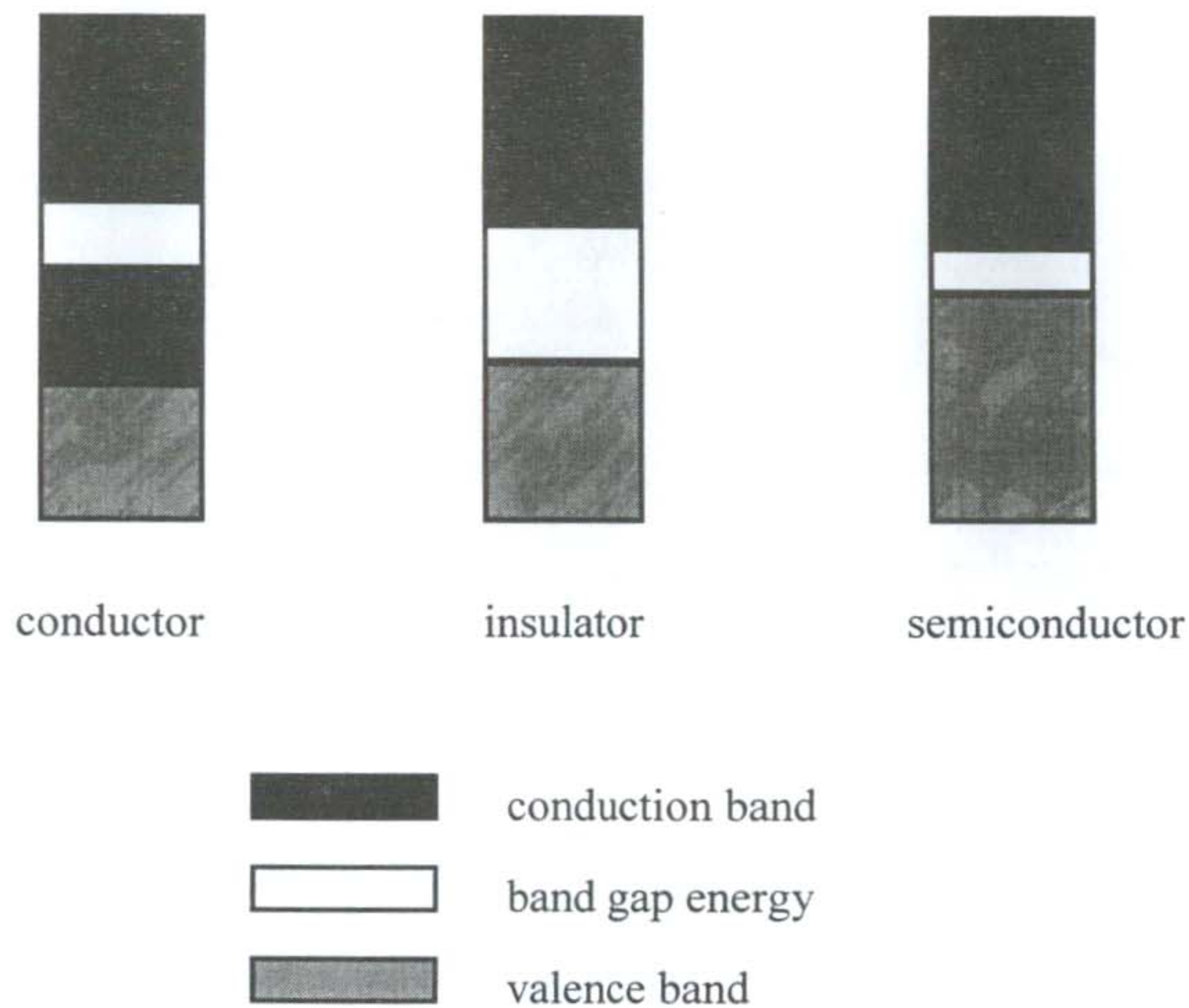


Fig. 2.1 Energy level band diagrams for three types of solids

In a conductor, the VB and CB overlap, and electrons can easily move to the CB without any energy input. Within that band, they can flow freely from atom to atom in

the solid. In insulators and semiconductors, the VB is separated from the CB by the band gap energy zone. In order for electrons to move to the CB and subsequently move from atom to atom within the solid, an external energy input equal to or greater than the band gap energy must be applied. The difference between an insulator and a semiconductor is a matter of degree. As a rule of thumb, a material is considered to be an insulator if the band gap energy is greater than about 3.5 eV and to be a semiconductor when it is less than 3.5 eV (Wang 1989).

Photoactive catalysts are semiconductors primarily composed of metal oxides. Table 2.2 lists several different photoactive semiconductors; their band gap energies vary widely, ranging from 2.2 eV to 3.5 eV. The equivalent wavelength is the wavelength of a photon that has energy equal to the band gap energy. The table shows that photoactivation of the anatase crystalline form of TiO_2 , for example, requires light of wavelengths less than or equal to about 413 nm.

Semiconductors typically used in solar energy applications and oxidation processes are categorized as n type semiconductors because it is very photoactive and stable in comparison to other semiconductors. Figure 2.2 illustrates the relative electron potentials for a heterogeneous mixture containing an aqueous solution and an n type semiconductor powder. The relative electron potential of the semiconductor and the redox potential of the solution are shown before and after contact in the presence of an external energy source. The Fermi energy level, E_f , represents the electrochemical potential of the solid. E_f is a statistical average of the total electron energy, which depend on the occupation of the valence and conduction bands. For an intrinsic

semiconductor, E_f lies between the energy levels of the the valence and conduction bands. Before contact between the photocatalyst and an aqueous solution, the conduction band and Fermi level of the semiconductor lie above the redox potential of the aqueous solution E_{redox} as shown in Fig. 2.2(a). However, after contact the Fermi energy level of the semiconductor and the redox potential of the solution reach the same potential equilibrium.

Table 2.2 Summary of several semiconductors and their band gap energies and wavelength of light energy equivalent to the band gap

Semiconductor	Type	Band gap (eV)	Equivalent wavelength (nm)
SnO ₂	N	3.50	354
KTaO ₂	N	3.50	354
SrTiO ₃	N	3.40	365
Nb ₂ O ₅	N	3.40	365
ZnO	N	3.35	370
TiO ₂ (anatase)	N	3.20	413
SiC	P	3.00	376
V ₂ O ₅	N	2.80	443
WO ₃	N	2.70	459
CdS	N	2.40	516
GaP	P	2.30	539
CdO	N	2.20	563

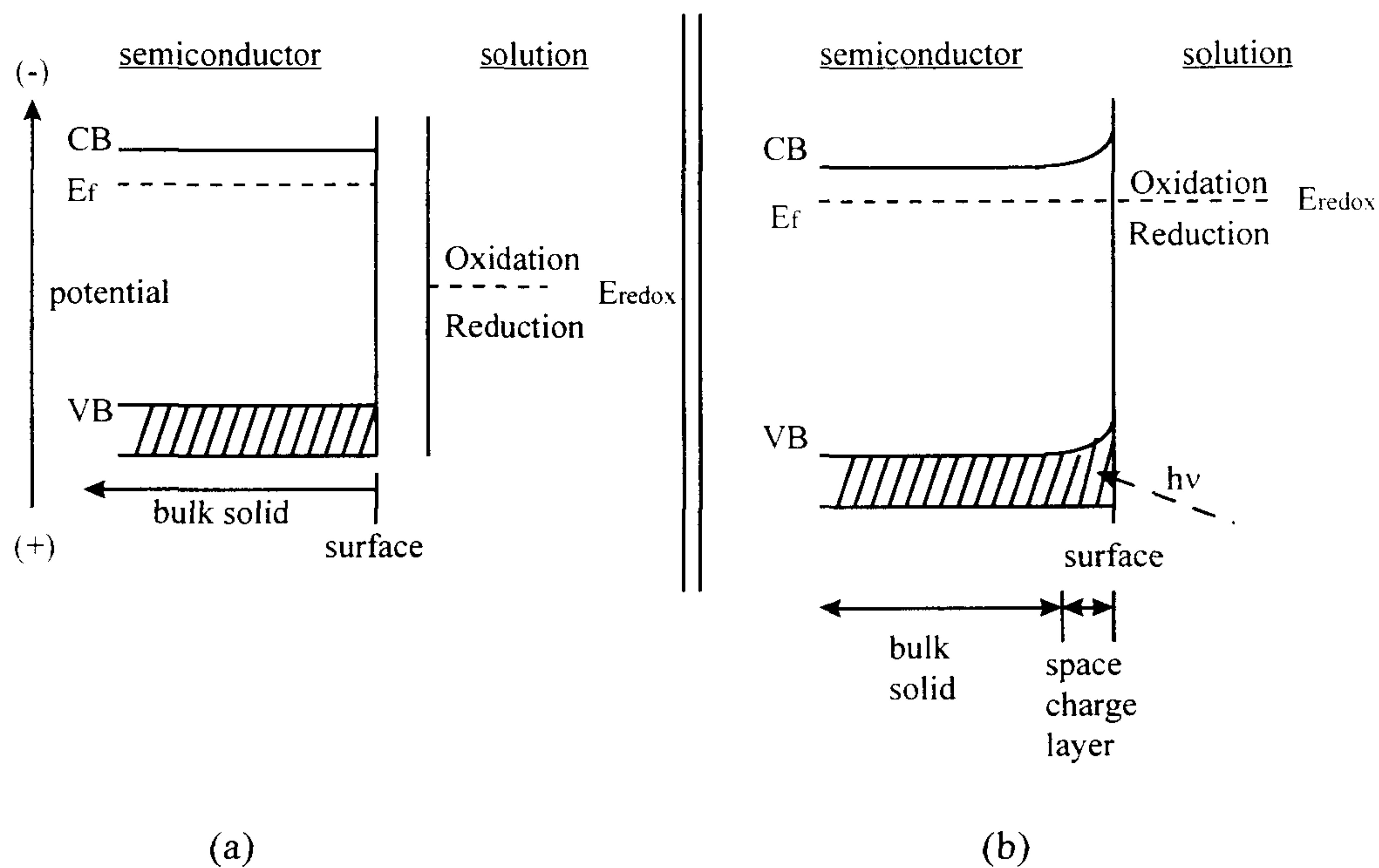


Fig. 2.2 Relative electron potential of a photocatalyst and redox potential of an aqueous solution: (a) electronic equilibrium before contact of catalyst and solution; (b) electronic equilibrium after contact

This equilibrium involves a depletion of the mobile conduction band electrons from the region at or near the semiconductor surface. The depletion causes a potential gradient near the solid-liquid interface, which bends the energy bands as illustrated in Fig. 2.2(b). The region in which this band bending occurs is referred to as the space charge layer. The depletion of the conduction band electrons in the space charge layer region can be caused by a reaction of the electrons with adsorbed molecules on the semiconductor surface or by electron-hole recombination reactions. In addition, surface defect sites in the semiconductor lattice may trap the electrons long enough for them to undergo chemical reactions.

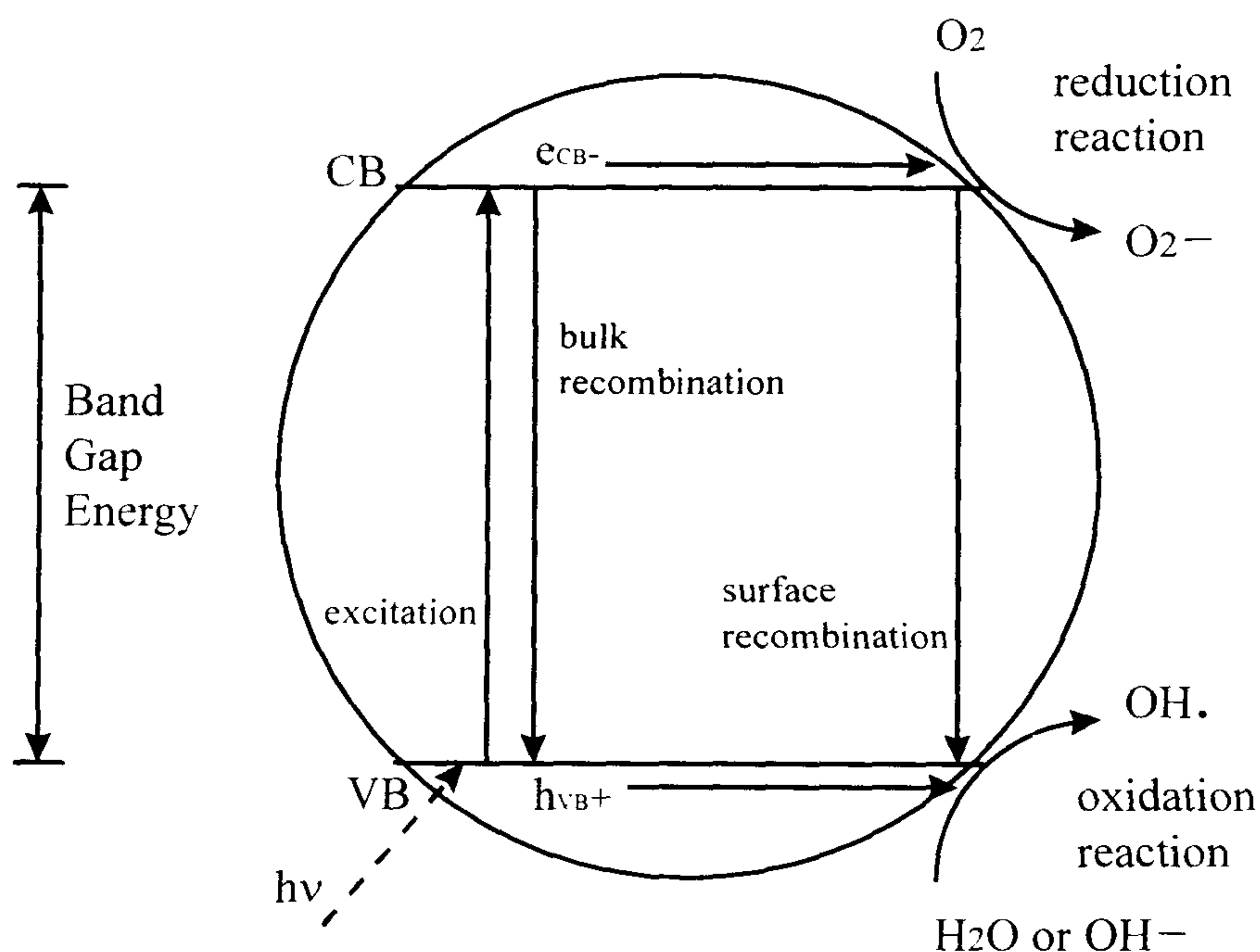


Fig. 2.3 Simplified schematic of the photoactivation mechanisms of an intrinsic semiconductor

The primary oxidant responsible for the photoassisted catalytic oxidation of organic compounds in aqueous solutions is the highly reactive hydroxyl radical. A simplified illustration of the mechanism for photoactivation of a semiconductor is presented in Fig. 2.3. In the simplest case of an intrinsic semiconductor, absorption of a photon of band gap energy or greater excites an electron (e_{CB}^-) to the conduction band while leaving an electronic vacancy (called a hole, h_{VB}^+) in the valence band.

A potential exists between the interior bulk solid and the external surface of the solid because of the depletion of conduction band electrons in the space charge region. The resulting gradient causes the photoexcited hole and electron to migrate to the exterior surface. In the absence of an electrical circuit, at steady state, the electron-hole pairs at the surface can recombine, producing only luminescence, or can react with adsorbed species on the surface to produce redox reactions. The redox reactions produce hydroxyl radicals (OH^\cdot) that are responsible for the oxidation of the organic compounds.

As described previously, we already have known that a semiconducting photocatalyst along with the absorption of light of suitable wavelength is a prerequisite for the complete decomposition of toxins present in water. Photoexcited semiconducting photocatalysts lead to light induced redox processes due to their electronic structure consisting of a filled valence band and an empty conduction band. Electron (e_{CB}^-) / hole (h_{VB}^+) charge pairs are generated within the photocatalyst particle following the absorption of photons with an energy exceeding the semiconductor bandgap energy.

If these charge carriers reach the semiconducting particle surface before they recombine they can be transferred to electron acceptor or donors, respectively, thus initiating the desired redox chemistry. Unless these e_{CB}^- and $h\nu_B^+$ charge carriers are involved in redox reactions immediately, they recombine and liberate heat in nanoseconds. Therefore, one way to improve the efficiency of the process is to retard the $e_{CB}^- - h\nu_B^+$ recombination rate by adding an irreversible electron acceptor such as platinum islands on the surface of TiO_2 .

Another trials to improve the relative photocatalytic efficiency is to modify pure TiO_2 by synthesizing the mixed oxide such as Ti/Fe, Ti/Zn, and Ti/Ni. Thus in this work we aimed at synthesizing the small particle of photocatalyst to investigate the effect of particle size on band gap energy in detail.

Recently, there has been a growing interest in ultrasmall particles that fall into the transition range between molecular and bulk properties (i.e. with diameters from 1 to 10 nm). Bulk semiconductors exhibit a pronounced increase in light absorption when photon energies exceed the band gap energy; however, the photophysics of ultrasmall semiconductor particles is substantially different. Quantum mechanical calculations (Brus 1983, 1984, 1986) and experimental observations (Ekimov and Onushchenko 1981, 1984; Ekimov et al. 1985) suggest that the energy level of the first excited state of the exciton increases with decreasing particle size thus leading to a blue shift in the absorption spectrum.

Several excellent review articles have been published recently concerning the

photophysical properties of these quantum sized semiconducting particles. In the following, we shall describe experimental observations noted during the synthesis of ultra-small metal oxide particles. Since the ISFH has been actively engaged in the investigations of quantum size metal oxide particles over the last six years, it will give KIER a great opportunity to learn about synthesizing technique and analysis. Besides their fascinating photophysical properties, the interest in small semiconductor particles suspended in aqueous solution originates in their unique photocatalytic properties. Here, we shall also make the attempt to illustrate and compare the photocatalytic activity of four different ultra-small metal oxide particles, i.e., TiO₂, Ti/Fe, Ti/Zn and Ti/Ni.

2.3 Photoreactors for solar application

The artificial generation of photons required for the detoxification of polluted water is the most important source of costs during the operation of photocatalytic wastewater treatment plants. This suggests to use the sun as an economically and ecologically sensible light source. With a typical UV- flux near the surface of the earth of 20 to 30 W/m² the sun puts 0.2 to 0.3 mol photons/m²hr in the 300 to 400 nm range at the process disposal. Principally these photons are suitable for destroying water pollutants in photocatalytic reactors.

In the wavelength range which can be used for the excitation of TiO₂ (UVA, 300-400 nm) the diffuse { $E_{dif}(300-400)=24.3 \text{ W/m}^2$ } and direct { $E_{dir}(300-400)=25.0 \text{ W/m}^2$ }

portion of the solar radiation (AM=1.5) reaching the surface of the earth are almost equal. This means that a light concentrating system can generally employ only half of the radiation available in this particular spectral region. In order to ensure efficient conversion of the incident photons to charge carriers the design of a solar reactor has to be considered and optimized. One example is followed.

The parabolic trough reactor (PTR) concentrates the sunlight into a focal line using parabolic mirrors. Light concentration up to a factor of 50 is achievable by standard PTRs. Hence only the direct portion of the solar spectrum is exploited. The parabolic trough reactor set-up at KIER, Korea and the Plataforma solar de Almeria (PSA) used for our experiments consisted.

Chapter 3. Experimental

3.1 Synthesis of mixed oxide photocatalyst

(1) Ti/Fe Mixed Oxide

The Ti/Fe mixed oxide colloids with different iron content of 2.5, 10, 20, 50 wt% were prepared as powders, which were stable at room temperature for several months and could be resuspended in water or water/ethanol mixtures yielding transparent colloidal solutions.

For the preparation of Ti/Fe mixed oxide colloids freshly distilled TiCl_4 (Yakuri Pure Chem. Co.) cooled to $-20\text{ }^\circ\text{C}$ was added slowly to cold ($\sim 0\text{ }^\circ\text{C}$) freshly prepared $\text{FeCl}_3 \cdot 6\text{H}_2\text{O}$ (Showa Chemical Inc.) solution under vigorous stirring. It was the intention of this preparation to thoroughly incorporate Fe^{3+} into the growing particles. In order to prove this, samples of colloidal solutions have been precipitated and tested colorimetrically for Fe^{3+} ions after removal of solid material.

The resulting colloidal suspension was stable for several hours at temperatures below $5\text{ }^\circ\text{C}$. To increase the stability of the colloids and to facilitate powder formation during evaporation of the solvent, the ionic strength was subsequently reduced by dialyzing with a membrane (Spectra/Por membrane MWCO : 5-8,000) against pure water until a final pH between 2.5-3 was reached. Aliquots of 200 mL were dried with the aid of a rotary evaporator (25 mbar, $30\text{ }^\circ\text{C}$) (Buch Rotavapor R-114) as shown in Fig. 3.1. The residue was dried under higher vacuum (1 mbar) for one minute,

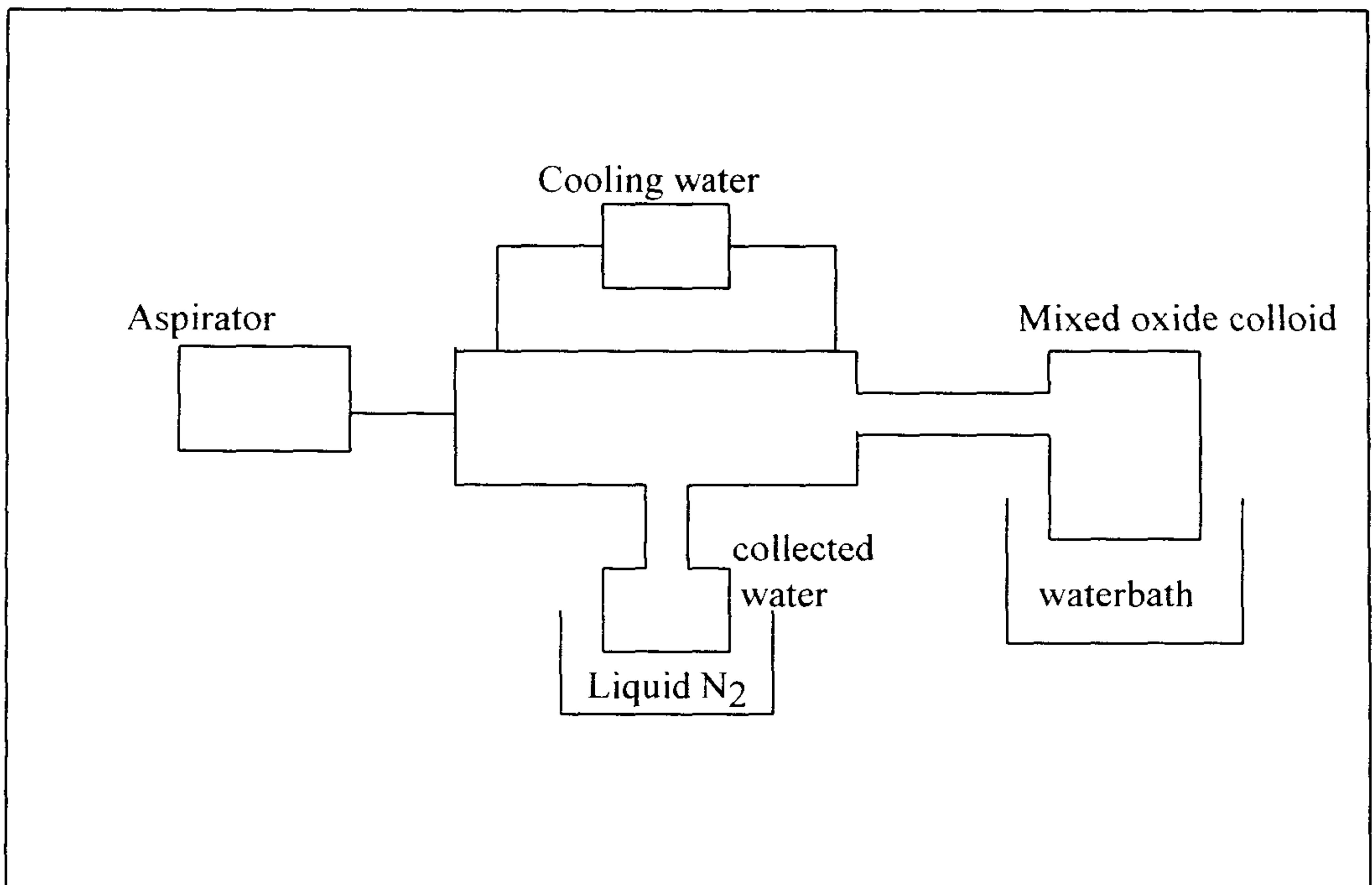


Figure 3.1 Schematic Diagram of Rotary Evaporator

resulting in crystalline yellowish to brownish powders. In these experiments deionized water ($> 18.2 \text{ M}\Omega\text{cm}$) by Milli-Q Plus was used.

Absorption spectra as a function of concentration of Fe ion and wavelength were observed by employing the UV-VIS spectrometer (Lambda 2, Perkin Elmer). Particle size analysis has been performed by TEM and EDAX analysis was employed to detect the actual Fe concentration in TiO_2 .

(2) Ti/Zn Mixed Oxide

The Ti/Zn mixed oxide colloids with different zinc content were prepared as powders, which were stable at room temperature for several months and could be resuspended in water or water/ethanol mixtures yielding transparent colloidal solutions.

For the preparation of Ti/Zn mixed oxide colloids freshly distilled TiCl_4 cooled to -20°C was added slowly to cold ($\sim 0^\circ\text{C}$) freshly prepared ZnCl_2 (Junsei Chemical Co.) solution under vigorous stirring. It was the intention of this preparation to thoroughly incorporate Zn^{2+} into the growing particles. In order to prove this, samples of colloidal solutions have been precipitated and tested colorimetrically for Zn^{2+} ions after removal of solid material.

The resulting colloidal suspension was stable for several hours at temperatures below 5°C . To increase the stability of the colloids and to facilitate powder formation during evaporation of the solvent, the ionic strength was subsequently reduced by dialyzing against pure water until a final pH between 2.3-2.5 was reached. Aliquots of 200 mL were dried with the aid of a rotary evaporator (25 mbar, 30°C). The residue

was dried under higher vacuum (1 mbar) for one minute, resulting in crystalline yellowish to brownish powders.

Particle size analysis has been performed by TEM and EDAX analysis was employed to detect the actual Zn concentration in TiO_2 .

(3) Ti/Ni Mixed Oxide

The Ti/Ni mixed oxide colloids with different nickel content were prepared as powders, which were stable at room temperature for several months and could be resuspended in water or water/ethanol mixtures yielding transparent colloidal solutions.

For the preparation of Ti/Ni mixed oxide colloids freshly distilled TiCl_4 cooled to -20°C was added slowly to cold ($\sim 0^\circ\text{C}$) freshly prepared $\text{NiCl}_2 \cdot 6\text{H}_2\text{O}$ (Junsei Chemical Co.) solution under vigorous stirring. It was the intention of this preparation to thoroughly incorporate Ni^{2+} into the growing particles. In order to prove this, samples of colloidal solutions have been precipitated and tested colorimetrically for Ni^{2+} ions after removal of solid material.

The resulting colloidal suspension was stable for several hours at temperatures below 5°C . To increase the stability of the colloids and to facilitate powder formation during evaporation of the solvent, the ionic strength was subsequently reduced by dialyzing against pure water until a final pH between 2.3-2.5 was reached. Aliquots of 200 mL were dried with the aid of a rotary evaporator (25 mbar, 30°C). The residue was dried under higher vacuum (1 mbar) for one minute, resulting in crystalline

yellowish to brownish powders.

Particle size analysis has been performed by TEM. Besides, each of different composition mixed oxides was prepared by theoretical calculation. To compare the theoretical composition with the obtained one, EDAX analysis for Fe/Ti was performed. EDAX analysis was employed to detect the actual Fe concentration in TiO₂.

As well, a couple of pure titanium dioxide, P25 from Degussa and Hombikat from Sachtleben Chemie GmbH were obtained and used as received. All bench-scale reactions were carried out in annular reactor equipped with a motor-driven peristaltic pump (Cole-Palmer Co.), Teflon tubing, and Pyrex sampling vessels.

3.2 Measurement of photonic efficiency

The photocatalytic activities of the mixed oxide particles were tested with detoxification measurements using 0.1 mM DCA as the probe molecule. According to equation (1), the oxidation of one DCA molecule leads to the formation of one proton. Therefore we used a pH-stat technique which allows the in-situ measurement of H⁺_{aq} formed during the photolysis experiment with extremely high sensitivity. The data from the autotitration system were transferred to a computer which calculates the concentration of the generated protons from the amount of the added base with respect to the elapsed time. Corrections due to the dissociation equilibria of

simultaneously formed H_2CO_3 (as HCO_3^- at $6.3 < \text{pH} < 10.3$ and as CO_3^{2-} at $\text{pH} > 10.3$) have been considered in the computer program. The autotitration system (from Metrohm) as illustrated in Fig. 2.3 was connected to a combined pH electrode (from Metrohm). The titrant solution (0.01 or 0.1 N NaOH) was kept under Ar and calibrated weekly with 0.1 N HCl. The photochemical reactor was made of quartz glass and filled with 50 mL colloidal solution which was thermostated and vigorously stirred by a magnetic stirring bar.

3.3 Fourier Transformed Infrared Spectrometer (FTIR) Analyses

To compare the relative amount of hydroperoxide group (O-H stretching, 3250 cm^{-1}) on each mixed oxides, FTIR (MB-104 from BOMEM) was used and sample pellets were prepared with KBr at a fixed concentration. Used parameters were resolution of 4 cm^{-1} and scan numbers of 16.

3.4 Double sheet skin photoreactor (DSSR) for real wastewater treatment

The Double Sheet Skin Reactor (DSSR) was used for the treatment of real wastewater from a company. DSSR is consisted of a reservoir storage, a pump and UV radiation meter (Fig. 3.2). The water is pumped between reactor and storage in cycle mode. The flow rate of the pump is 9 l/min so that a homogeneous mixing of the

catalyst can be guaranteed. The system was placed outside to make real solar experiments with sunlight. The goal of this investigation is to test the applicability of this system to different kinds of real wastewaters. To find the maximum detoxification rate we used different kinds of catalysts (P25, Hombikat) with different concentrations (1g/l, 5g/l). The degradation was analyzed with TOC (Total Organic Carbon) analyzer (SHIMADZU 5000A) and COD (Chemical Oxygen Demand) analyzer (reactor with DR/2000 reader from HACH). Both are some standards for the pollution of the wastewater.

In this trial we tested the detoxification of real wastewaters from LG semiconductors, Korea. We received two different kinds of wastewaters. One contains a huge amount of H₂O₂ (H₂O₂), the other does organic pollutants (ORG). Detailed information is in table 3.1. In our first experiments we mixed the two waters hoping that the H₂O₂ water fastens the degradation of the organic compounds. Different catalysts were used for the treatment of wastewater at different concentrations and pH. After these experiments we worked with the ORG. Again we tried different catalysts.

In all experiments the total volume of wastewater in the system is 20 l, the reaction volume in the DSSR is 14 l. In all experiments the wastewater was diluted by a factor of 5. So in the presented figures the measured values are timed by a factor of 5. Because of this dilution factor the error range for TOC is about ± 10 ppm, for COD it is about ± 25 mg/l. Before taking samples in every experiment the water was mixed for about 1h after adding all components.

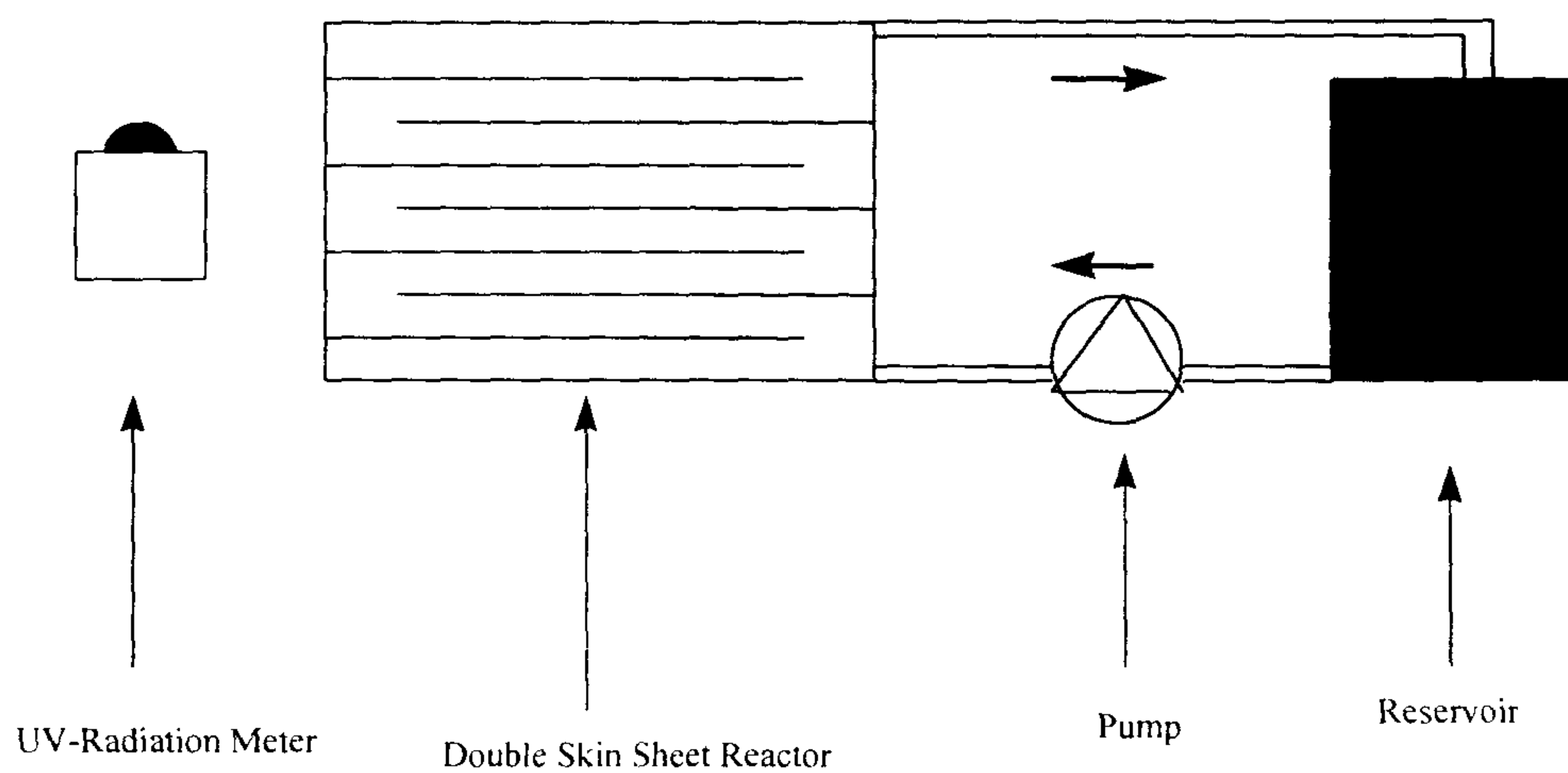


Fig 3.2. Schematic Diagram of Reactor system

Table 3.1. Chemical Data Sheet of the waste waters H₂O₂ and ORG and the mixed water. (values in brackets were measured in our Lab.)

	H ₂ O ₂	ORG	H ₂ O ₂ / ORG
Daily produced (1000 kg/day)	600	1000	-
PH	7~10 (10.1)	8~10 (11.1)	(10.3)
TOC (ppm)	- (0.95)	200 (869.5)	(415.2)
COD (mg/l)	1500 (557)	100 (882)	(705)
H ₂ O ₂ (mg/l)	3000	-	-
SS* (mg/l)	20	20	-

*SS : suspended solids

Chapter 4 Results and Discussion

4.1 UV/VIS absorbance

UV/VIS absorption spectra were drawn with a Ramda II UV/VIS spectrometer from Perkin-Elmer and the investigated range of wavelength was 200 ~ 800 nm. Measurements were performed for samples taken while aging, at the end of aging, and at one hour after solution of each mixed oxide was made.

UV/VIS absorbance measurements were conducted for samples taken at three different stages described in previous section 2.1. At first, results from samples taken while dialyzing are shown in figure 4.1 ~ 4.3. For Fe/Ti was red-shifted absorbance surely happened with increasing Fe content. In the cases of Ni/Ti and Zn/Ti, however, absorbancies were blue shifted as each content was increased. These results are consistently proven with colloids (figure 4.4 and 4.5), and DCA degradation efficiency (figure 4.6 and 4.7) where added amount of NaOH decreased with content of Ni and Zn increased. Calculated photonic efficiencies are in figure 4.8 and 4.9. Zn/Ti samples showed higher efficiency except for 50% content, while Fe/Ti resulted in much higher photonic efficiency (figure 4.9). This can be explained by red-shift of this mixed oxide.

4.2 Actinometry

Measuring the light intensity (I) of xenon lamp used (High pressure 600W xenon lamp) is essential to obtain the photonic efficiency. Standard solution with

Aberchrome 540 from Aberchromic Ltd. was prepared at the concentration of 5 mM. At 494 nm UV/VIS absorbance of this solution was measured after repeated illumination for 10 seconds. The optical pathway contained a shutter and a W/WG 320, a GG445, and a UG 5 filter to eliminate radiation with wavelengths shorter than 320 nm. The slope of graph (absorbance vs. time) was inserted into following equation A.1. to obtain the light intensity for our system.

$$I = \frac{\text{slope}}{8200 \times 0.2} \quad [\text{mole photons}/L \cdot s] \quad (\text{A.1.})$$

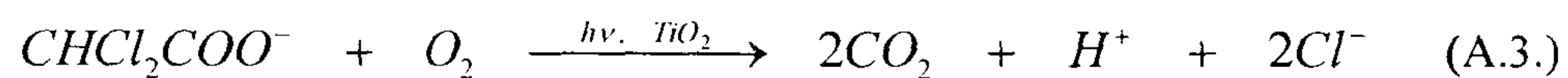
where slope is from the graph of absorbance vs. time.

4.3 DCA degradation and photonic efficiencies

Using 'pH-stat' method with a 614 Impulsemate, 713 pH meter, and 665 Dosimat from Metrohm Co. and xenon lamp as a light source, produced concentration of H⁺ in DCA degradation reaction was calculated by added 0.01N NaOH solution. Added amount of NaOH was tracked and collected via on-line computer. Reactor volume was 80 ml and was made of quartz. Reaction temperature was kept constant with cooling water. After determining light intensity (*I*), the photonic efficiency can be determined using equation A.2.

$$\text{Photonic Efficiency} = \frac{[\Delta H^+]/\Delta t}{I \text{ (intensity)}} \quad (\text{A.2.})$$

DCA is a relatively strong acid and in aqueous solution present in the form of anion irrespective of pH. Also, this substance is known to be photocatalytically degraded as follows (A.3.).



For Fe/Ti mixed oxides concentration of H^+ increased as Fe content increased. This is because of aforementioned decreased bandgap energy, that is, absorbing the wide range of light wave length. For Ni/Ti as well as Zn/Ti, however, $[\text{H}^+]$ decreased as content of Ni and Zn increased due to the increased bandgap energy.

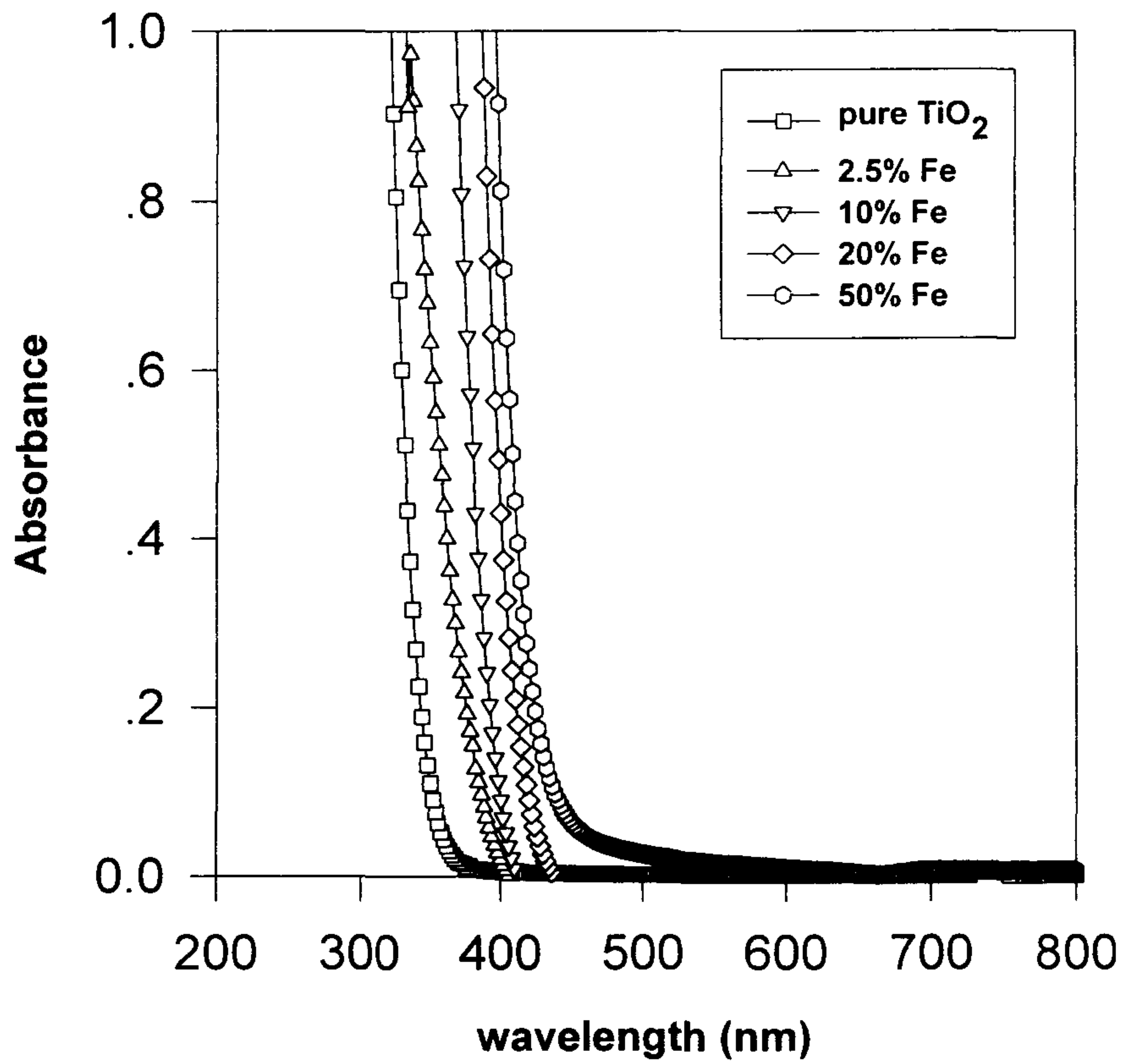


Figure 4.1 UV/VIS Absorbancies of Fe/Ti Samples while Dialyzing

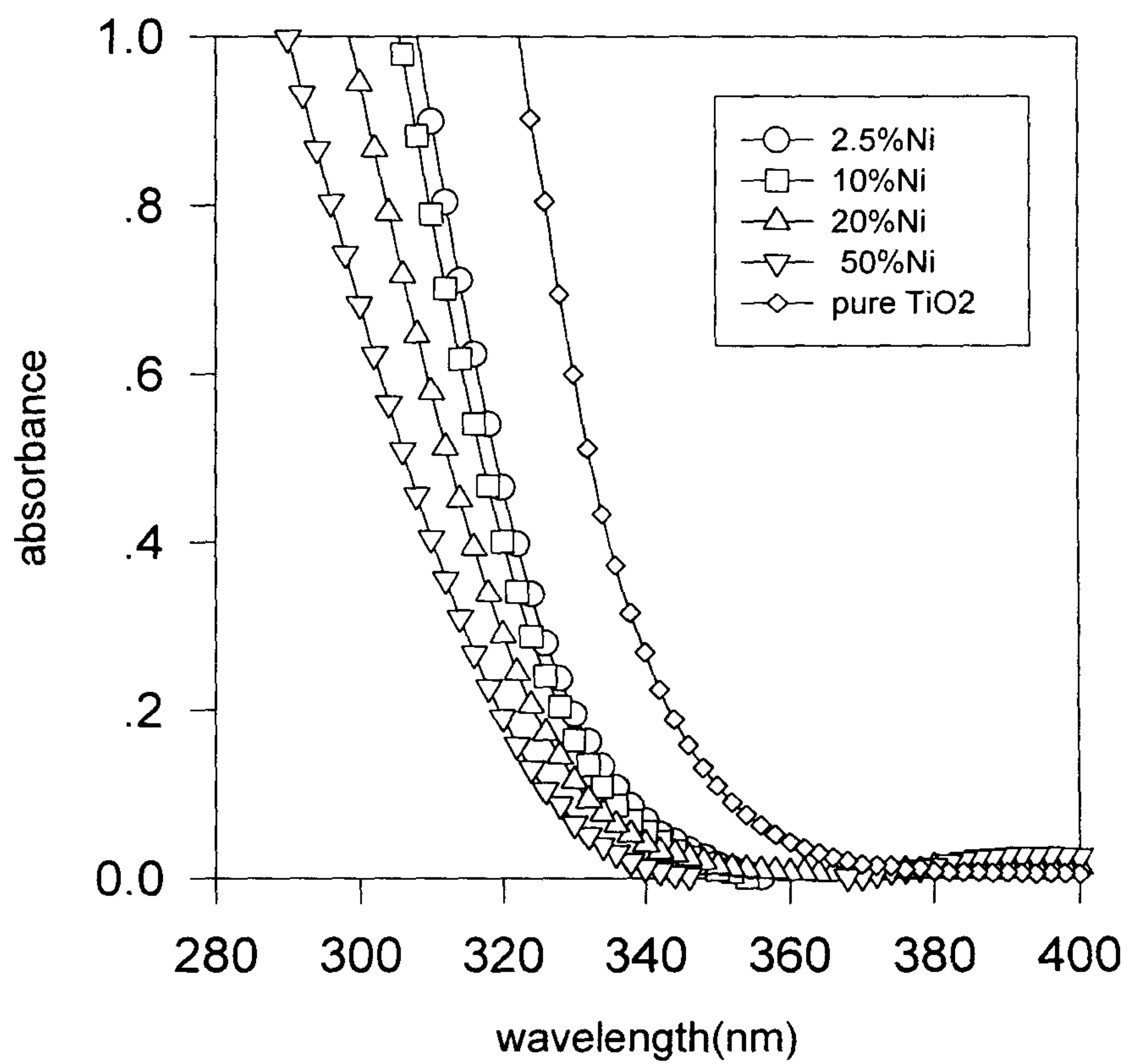


Figure 4.2 UV/VIS Absorbancies of Ni/Ti Samples while Dialyzing

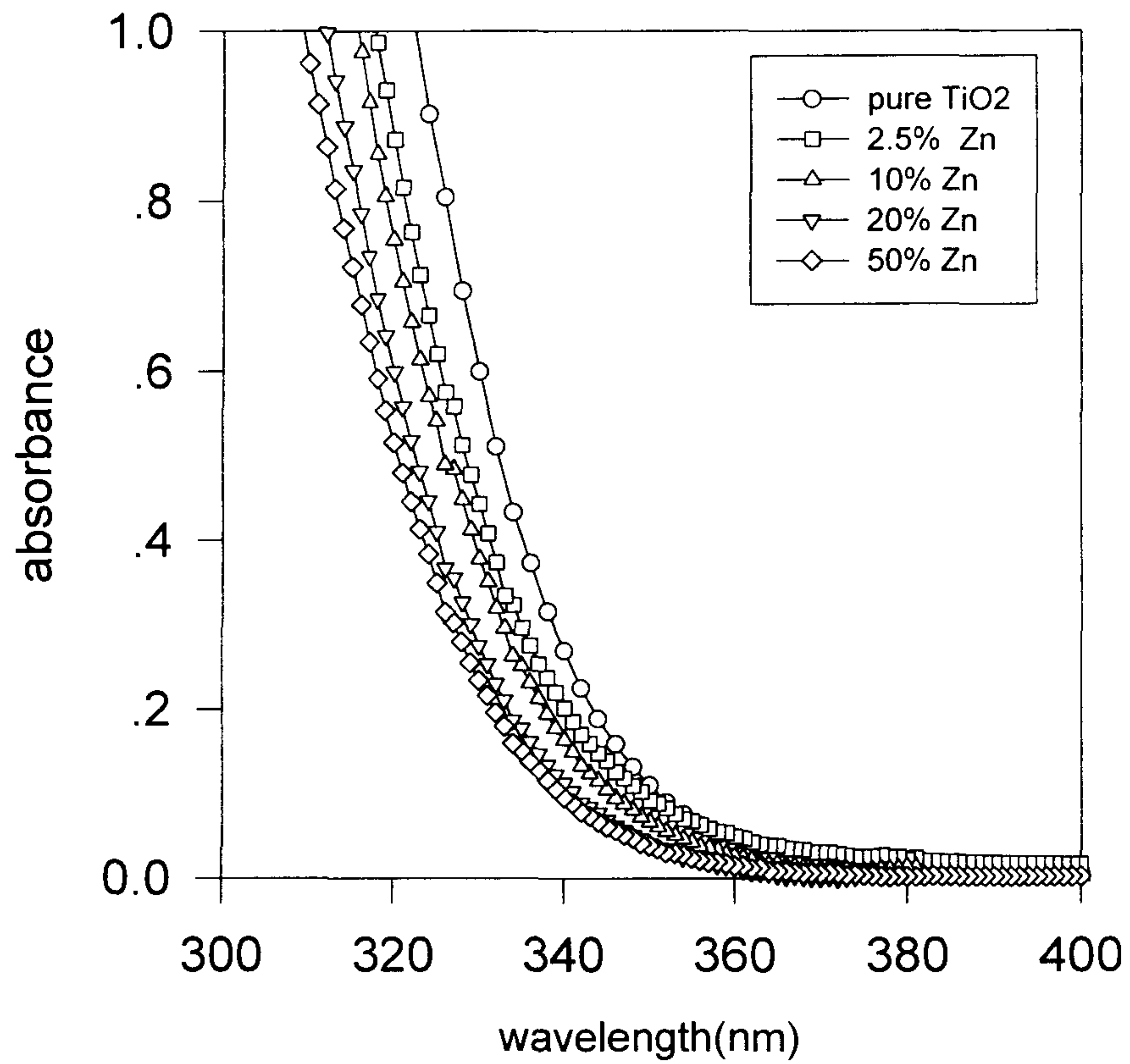


Figure 4.3 UV/VIS Absorbancies of Zn/Ti Samples while Dialyzing

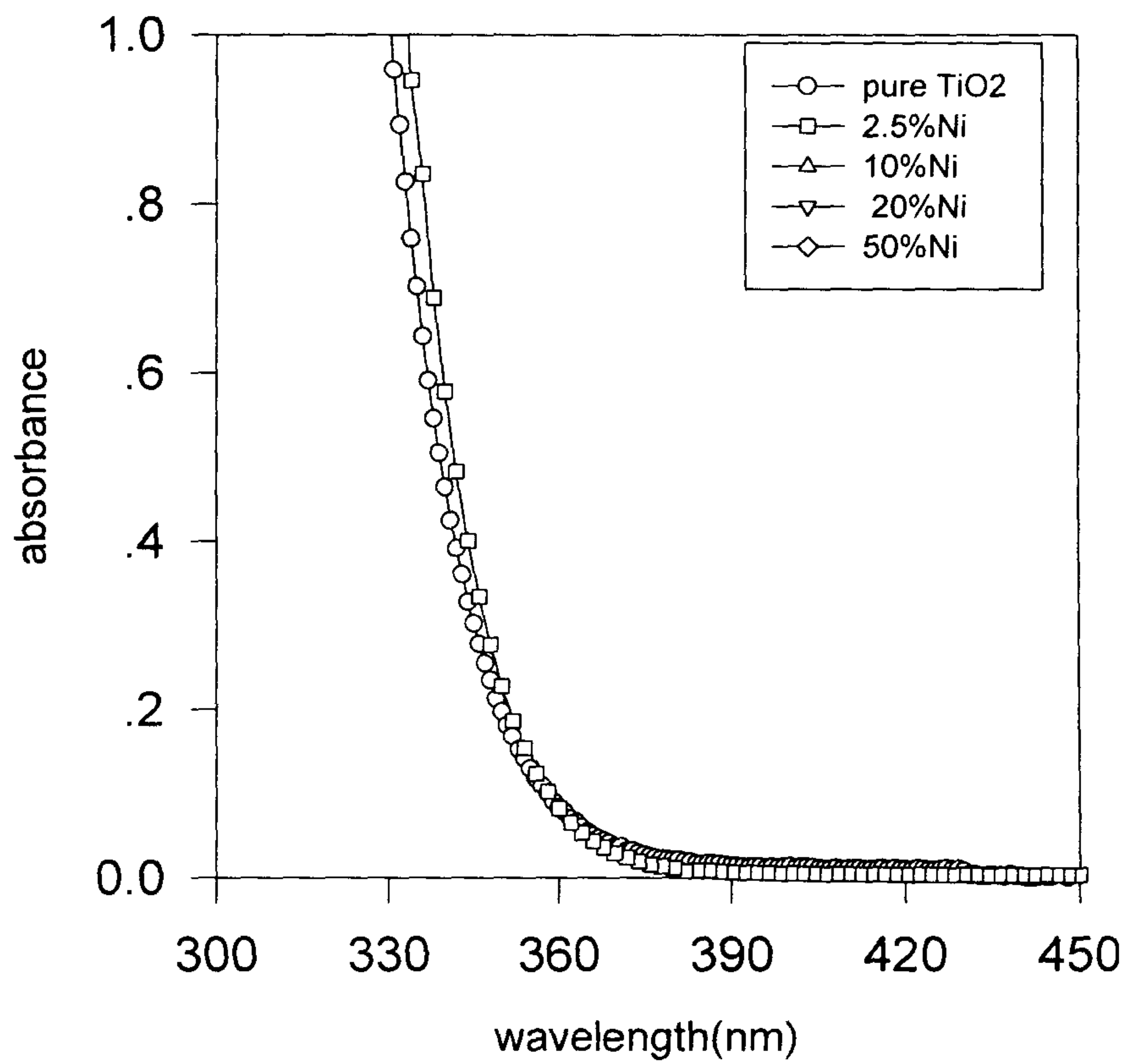


Figure 4.4 UV/VIS Absorbancies of Ni/Ti Colloids

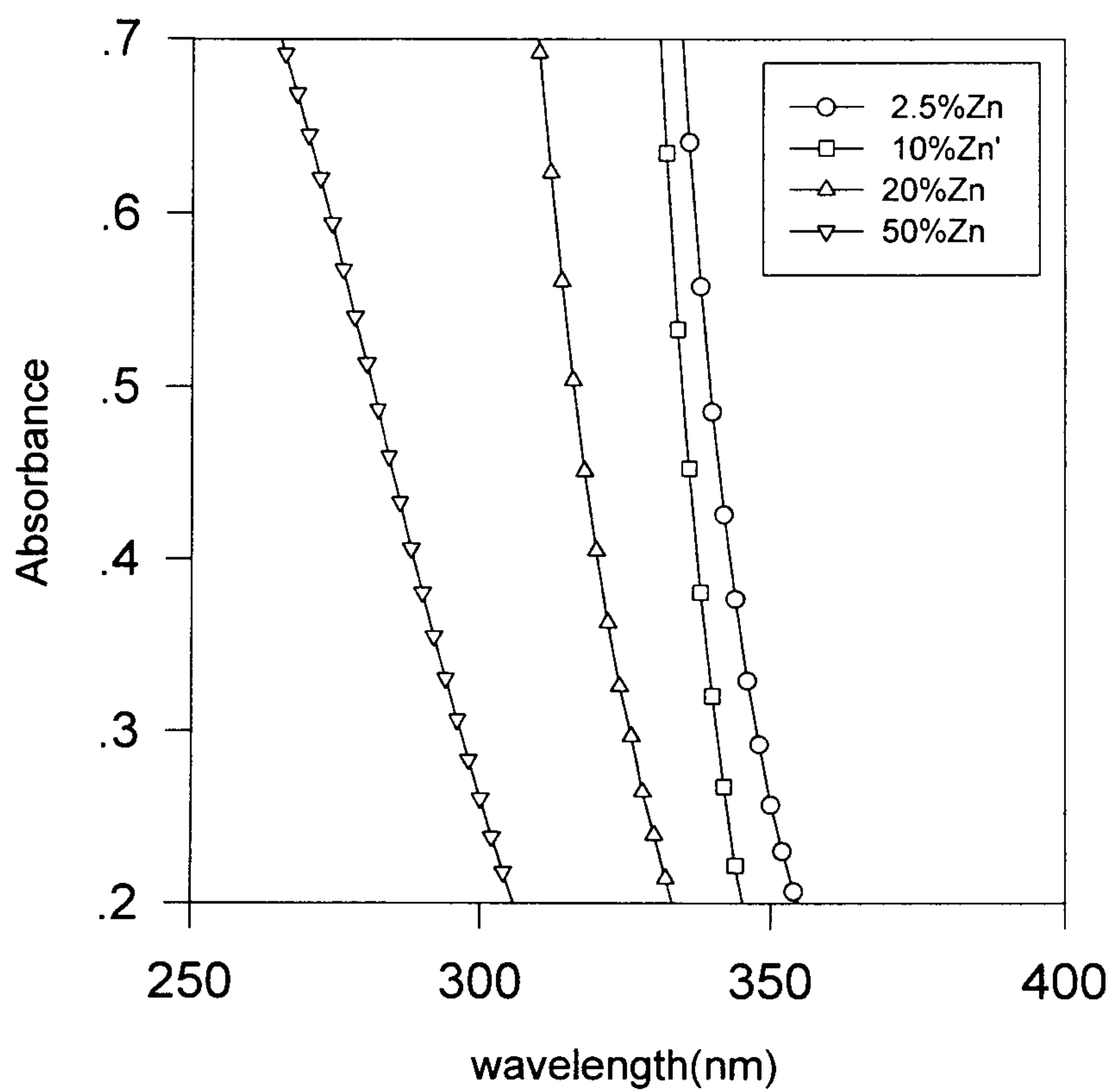


Figure 4.5 UV/VIS Absorbancies of Zn/Ti Colloids

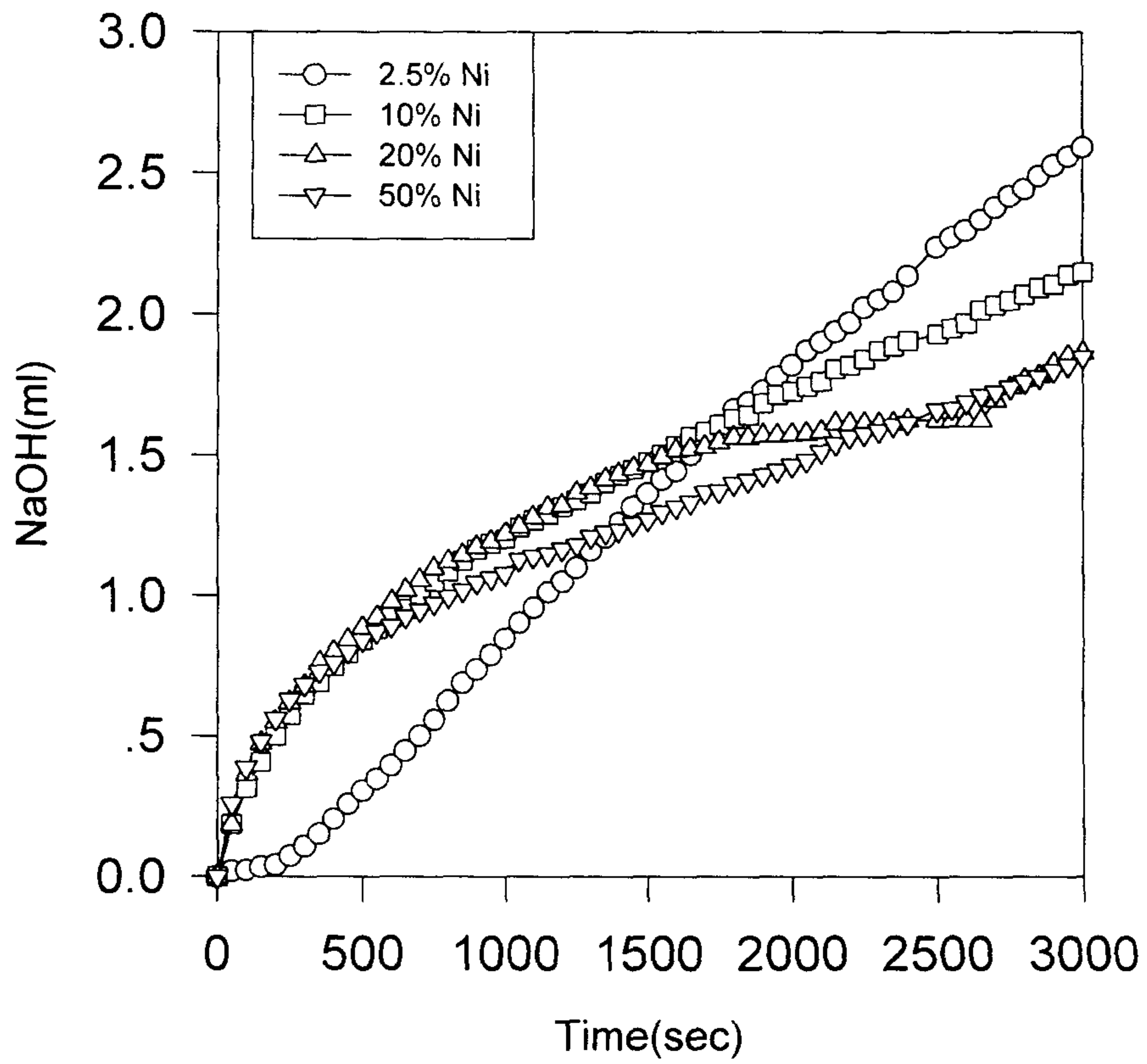


Figure 4.6 Amount of Added NaOH for degradation of DCA with Ni/Ti

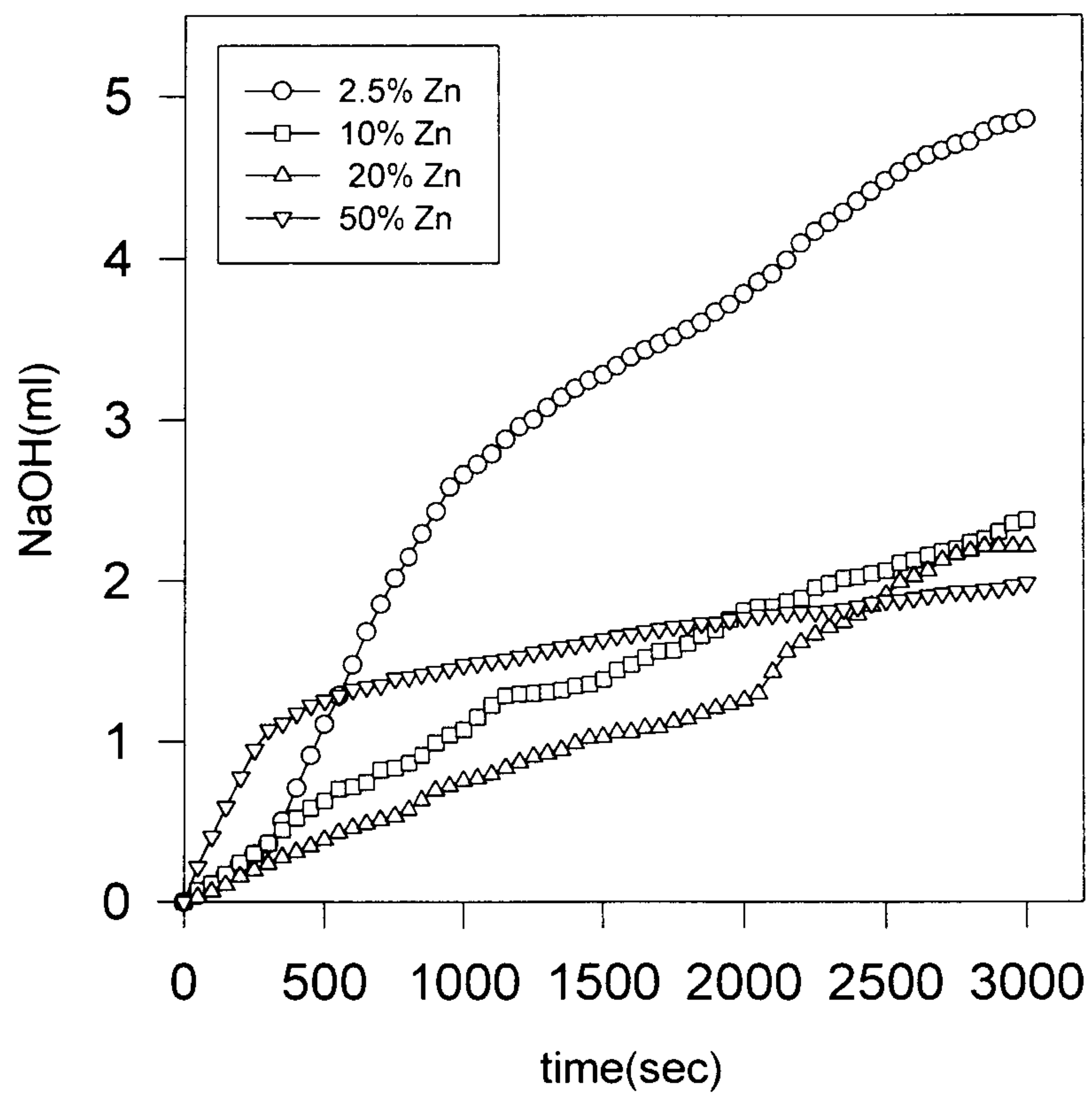


Figure 4.7 Amount of Added NaOH for degradation of DCA with Zn/Ti

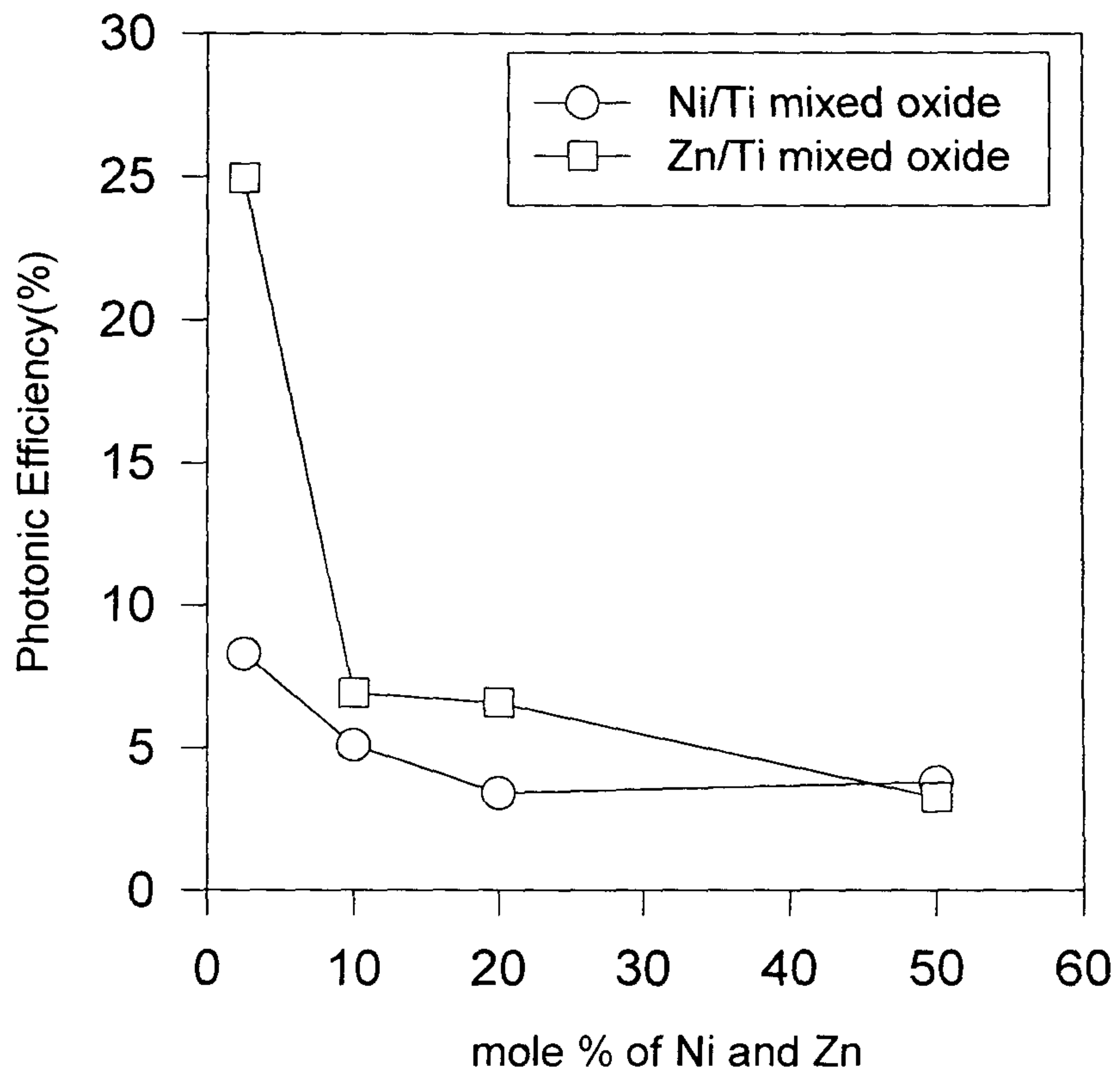


Figure 4.8 Comparison of Photonic Efficiency between Ni/Ti and Zn/Ti

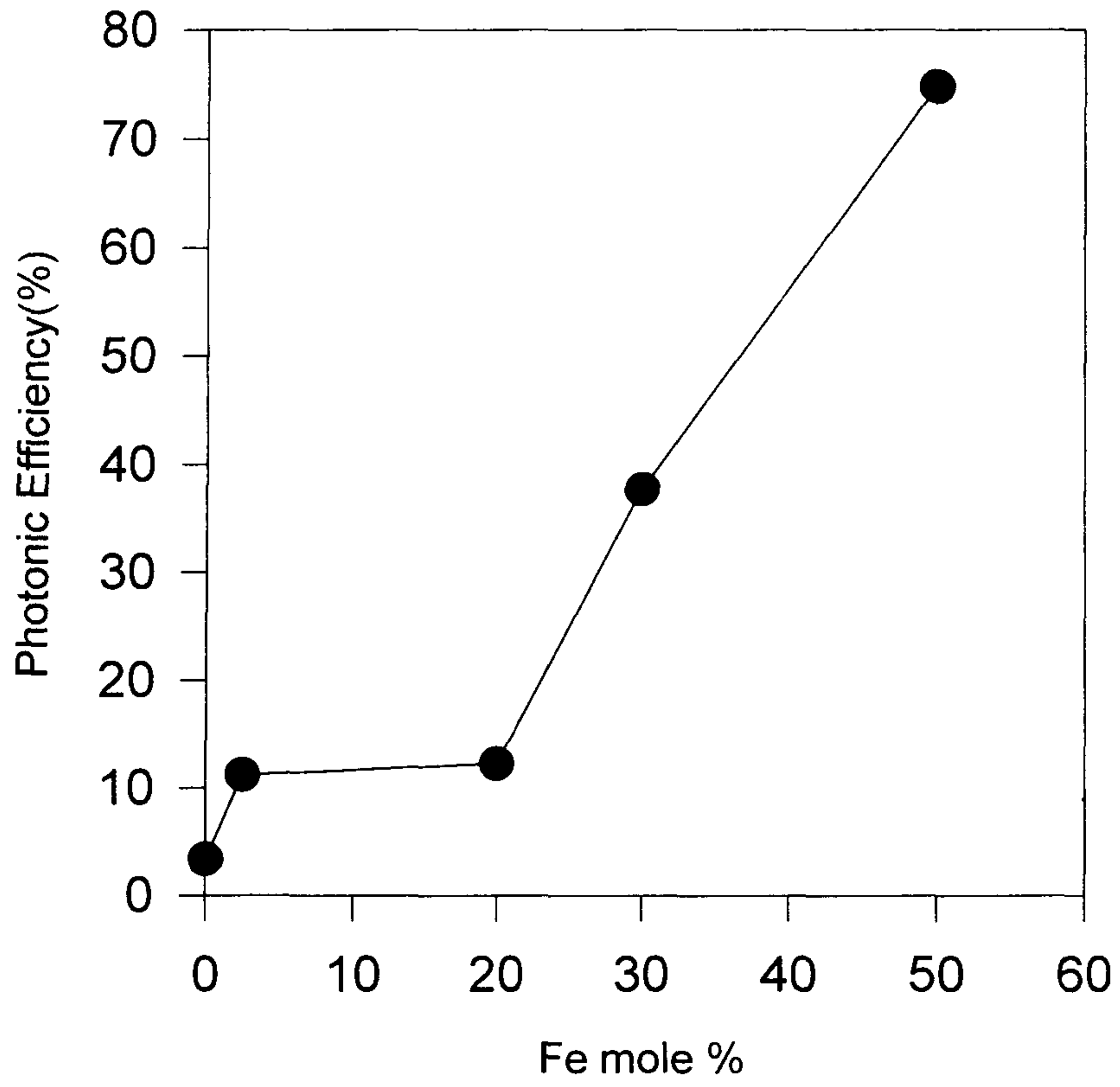


Figure 4.9 Photonic Efficiency for Fe/Ti

4.4 EDAX and Fourier transformed infrared spectrometer (FTIR)

Generally, results from EDAX were in good agreement with the theoretical values. However, chlorine was proven present at high concentration. This is attributed to the partial elimination of chlorine ion, which was produced during TiO₂ preparation (eq. A.4.) because dialyzing time was not long enough.



FTIR absorbance study was performed to envisage the capacity of adsorption of prepared mixed oxides. Spectra from FTIR analyses were in figure 4.10 ~ 4.12. For Fe/Ti, as the content of Fe increased the area under 3250 cm⁻¹ increased, while the others decreased. It was believed that these data indirectly represented the ability of producing the surface bouded Ti-OH groups.

File # 2 : FE50-1

Mode = 2 (Mid-IR)

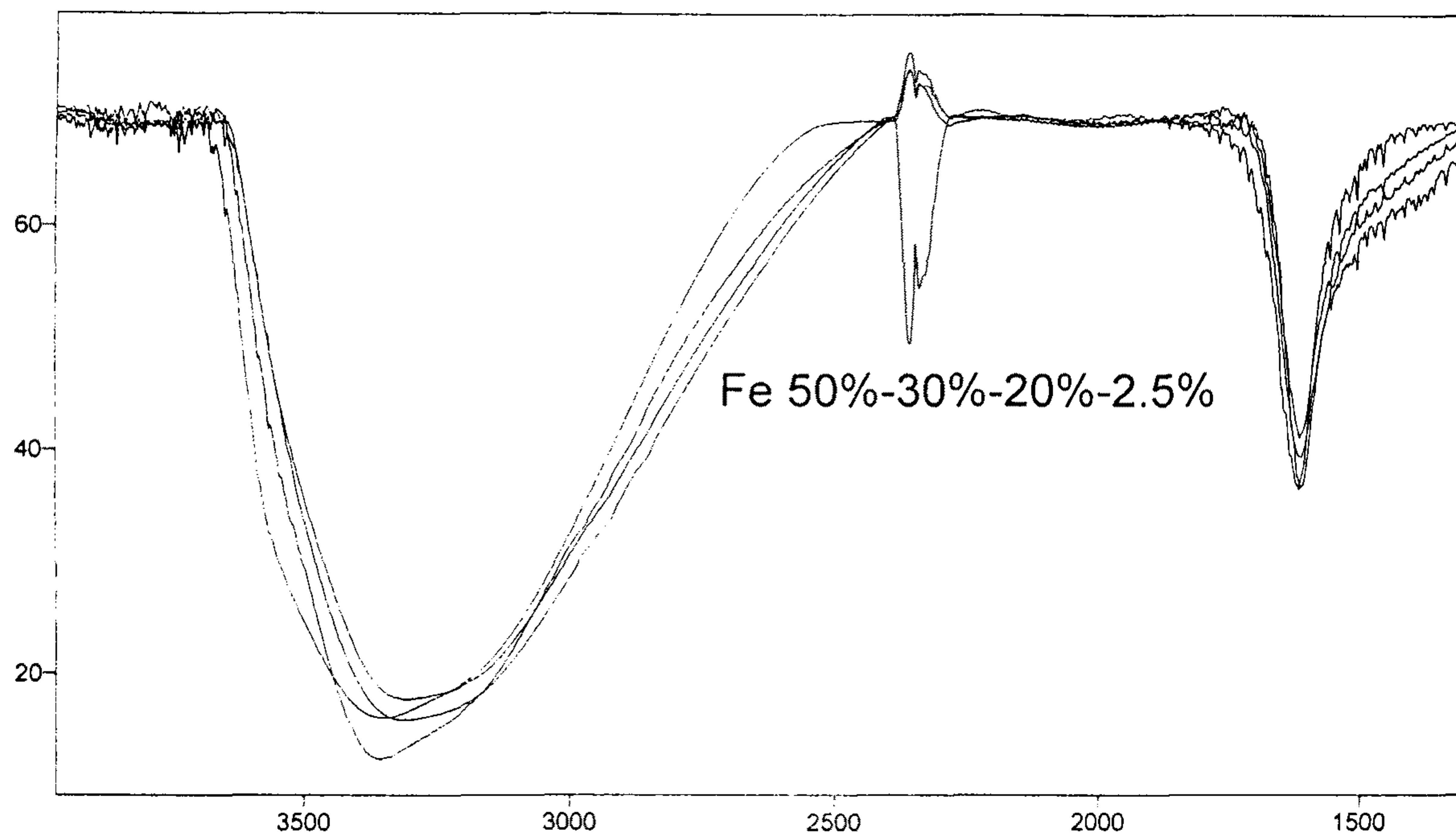
97/10/28 8:52 PM

Sample Description: MB104 \ ZnSe Beamsplitter \ DTGS with KRS-5 \KBr

Scans = 16

Res = 4 cm-1 20 scans/min

Apod = Cosine



Transmittance / Wavenumber (cm-1)

Figure 4.10

FTIR for Fe/Ti

File # 4 : ZN20

Mode = 2 (Mid-IR)

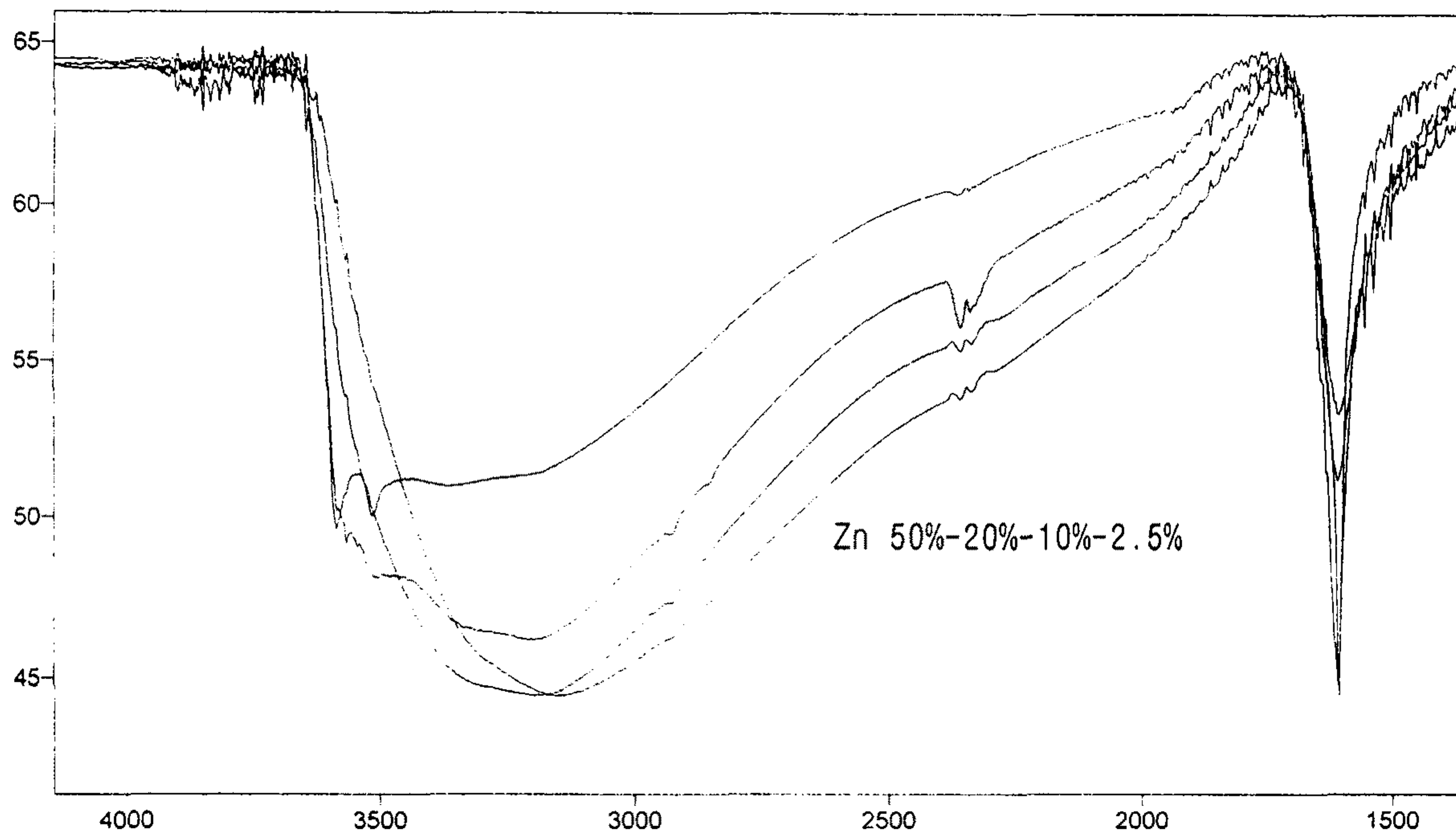
97/10/27 7:52 PM

Sample Description: MB104 \ ZnSe Beamsplitter \ DTGS with KRS-5 \KBr

Scans = 16

Res = 4 cm-1 20 scans/min

Apod = Cosine



Transmittance / Wavenumber (cm-1)

Figure 4.12

FTIR for Zn/Ti

4.5 Real wastewater (from LG semiconductor Co., Korea) treatment study

4.5.1. Double sheet skin reactor (DSSR); Mixing H₂O₂/ORG (1:1) without pH adjusting using different catalysts

We started with the mixed waters of H₂O₂ and ORG. The easiest (cheapest) way of using solar detoxification systems is without modification of wastewater. So we started experiments without pH adjusting using different catalysts and different catalyst concentrations. This H₂O₂ has been produced at the rate of 600 ton/day and ORG 1000 ton/day. Initial pH is in the range of 7 – 10. As a reference, followed are limitations of emission of wastewater in Korea effective from 1996, depending on the amount and area of wastewater produced.

Table 4.1 Emission limitations* in Korea

(mg/l)

Amount	More than 2000m ³ /day			Less than 2000 m ³ /day		
Area code	BOD	COD	SS	BOD	COD	SS
A	30	40	30	40	50	40
B	60	70	60	80	90	80
C	80	90	80	120	130	120
D	30	40	30	30	40	30

* from Korea Sustainable Development Network (KSDN).

A. 1g/l P25

The first experiment was carried out at the concentration 1g/l P25. The weather was quite sunny and it was represented in the UV data ranging from 1 to 4 mW/cm². The COD and TOC data were measured (Fig. 4.13). During the reaction time of 3.5 hour no degradation was seen in terms of TOC or COD.

B. 5g/l P25

The next experiment was with 5g/l P25 to find out the influence of catalyst concentration. Again the UV data show it was a quite sunny day (see Fig. 14). This time there was a slight decrease in TOC values by about 10 ppm within the experimental time of 4h. Also the COD data decreased about 50mg/l. But still these values are in the range of each error bars.

C. 5g/l Hombikat

To compare the influence of the catalyst this time we took 5g/l Hombikat. Again a slight decrease in TOC and COD was measured. TOC decreased about 20ppm, COD about 20 mg/l within the experimental time of 4.5h (see Fig. 15).

These experiments show clearly that the experimental time of about 4h is too short to find out the decomposition rates for these systems. To have an idea if something happens in these systems experiment with 4 days of running time was performed.

TOC and COD were only measured, not the UV data. Within this time scale decrease in TOC by about 220 ppm and in COD by about 150mg/l was observed (see Fig. 16). Hence, it is concluded that cleaning of the water without pH adjusting is possible but not very efficient due to very long running time.

4.5.2. Experiment on laboratory scale with H₂O₂ and 1g/l P25

Since the first experiments showed a very unsatisfying decomposition rate a laboratory scale experiment was carried out.

A. H₂O₂ water with 1g/l P25, pH 3 adjusting and oxygen input.

A UV-C lamp was used to generate the UV radiation. It can easily be seen that within the experimental time of about 3h the COD decreases nearly to zero (see Fig. 17). This strongly indicates the need of pH adjusting and perhaps also of oxygen input to get a sufficient waste water treatment. Therefore in the further experiments we used pH adjusting and an air compressor to increase the solved oxygen in the water.

B. Mixing H₂O₂ / ORG (1:1) with pH adjusting using Hombikat

Since Hombikat seems to be more efficient it was used in this experiment with pH adjusting and air compressor. Figure 18 shows a significant increase of the decomposition rates. Within the experimental time of 3h a decrease in TOC by about 120ppm and in COD by about 300mg/l was measured. This clearly shows the need of pH adjusting and perhaps also of oxygen input to yield high photonic efficiencies.

C. ORG with pH adjusting using different catalysts

To find out the influence of the H₂O₂ process water on decomposition rates the next experiments were carried out without H₂O₂ just using the organic waste water ORG. pH adjusting and air compressor were used to get high photonic efficiencies.

C.1. 5g/l Hombikat

Using Hombikat a decrease in TOC by about 150ppm and in COD by about 400mg/l was measured (see Figure 19).

C.2. 5g/l P25

With P25 decrease in TOC by about 250ppm and in COD by about 350mg/l was measured (see Figure 20).

4.5. 3. Comparison of the different detoxification methods

For the comparison of the different water treatment methods it is important to take into account the different solar irradiation data for each experiment. Hence a plot style UV energy input vs. TOC/COD is a more useful tool. Since all samples were taken in the same time distances (0.5h) it was the easiest way just to sum the UV Intensity data from sample to sample. So the puzzling unit mW/cm²*0.5h was created. In the following plots just the TOC vs. UV energy input is shown so that the plots are not too loaded with data.

A. Mixed H₂O₂/ORG with different catalysts without pH adjusting

Figure 21 shows the plot style UV energy input vs. TOC for the mixed water H₂O₂/ORG using different catalysts without pH adjusting. It can be seen that for 1g/l P25 the TOC remains constant. For 5g/l P25 there can be seen a slight decrease of the TOC with a negative slope of about 2.5 ppm/(mW/cm²*0.5h). For 5g/l Hombikat this negative slope is about 1.8 ppm/(mW/cm²*0.5h). So the P25 process is about 1.4 times more efficient than the Hombikat process. Though this comparison has to be taken carefully because the error bar of these slopes is about 1 ppm/(mW/cm²*0.5h).

B. Mixed H₂O₂/ORG with different pH

Here the influence of the pH is studied for the system H₂O₂/ORG using 5g/l Hombikat. In the experiment with pH 2.9 there was additional used an air compressor. It can clearly be seen that the pH 2.9 process is much more efficient than the pH 7.6 process (see Figure 22). In numbers the pH 7.6 process has a negativ slope of about 1.8 ppm/(mW/cm²*0.5h) but the pH 2.9 process of about 9 ppm/(mW/cm²*0.5h). Hence the pH 2.9 process is about 5 times more efficient.

C. ORG with different catalysts and pH adjusting

The influence of the catalyst on the decomposition of the pure ORG waste water is an interesting topic which is studied here. In both experiments pH adjusting and air compressor were used. Figure 23 shows that with Hombikat the TOC degrades with a negativ slope of about 15 ppm/(mW/cm²*0.5h) but with P25 it degrades with about

20 ppm/(mW/cm²*0.5h). So the P25 process is again about 1.3 times more efficient than the Hombikat process.

D. Influence of H₂O₂ on decomposition rate

For the application of the detoxification system it is an interesting question whether it is better to treat the mixed water H₂O₂/ORG or just the single waters, or in other terms which influence does the H₂O₂ water have on the degradation. Both experiments were carried out with 5g/l Hombikat, pH adjusting and air compressor. Figure 24 shows that the pure ORG water degrades with a negative slope of about 15 ppm/(mW/cm²*0.5h). The TOC data of the mixed water have a negative slope of about 9 ppm/(mW/cm²*0.5h). So the pure ORG process seems to be about 1.7 times more efficient. But one has to take into account the different initial TOC concentrations. If one assumes a first order kinetics in both systems, that means the degradation rate is proportional to the pollutant concentration, in fact the mixed system would be about 1.3 times more efficient. So this question can not be answered definitely with these data because we do not know anything about the kinetics. So these measurements have to be repeated with the same initial TOC concentrations.

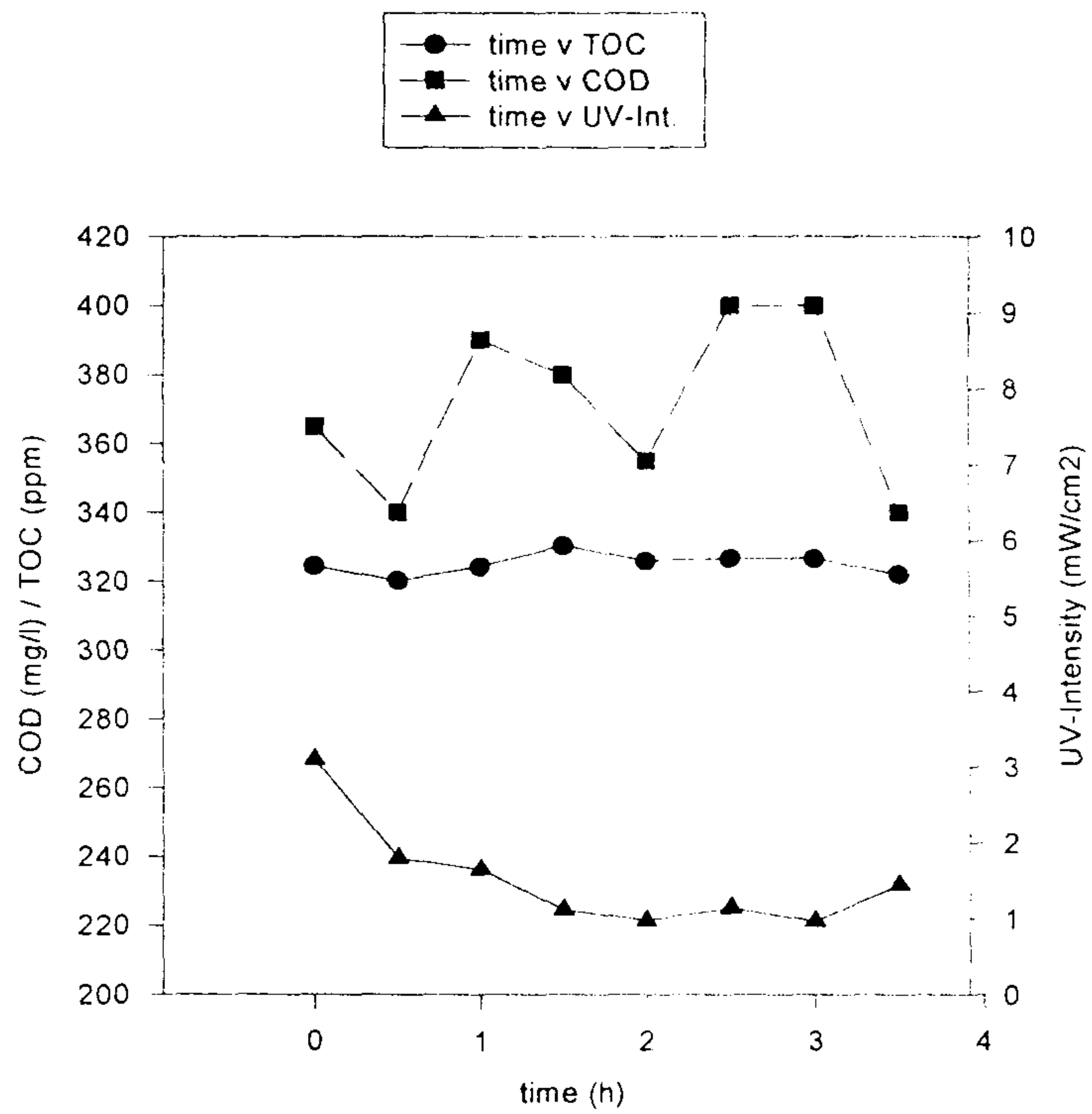


Figure 4.13 H_2O_2/ORG (1:1), 1g/l P25, pH=9.3

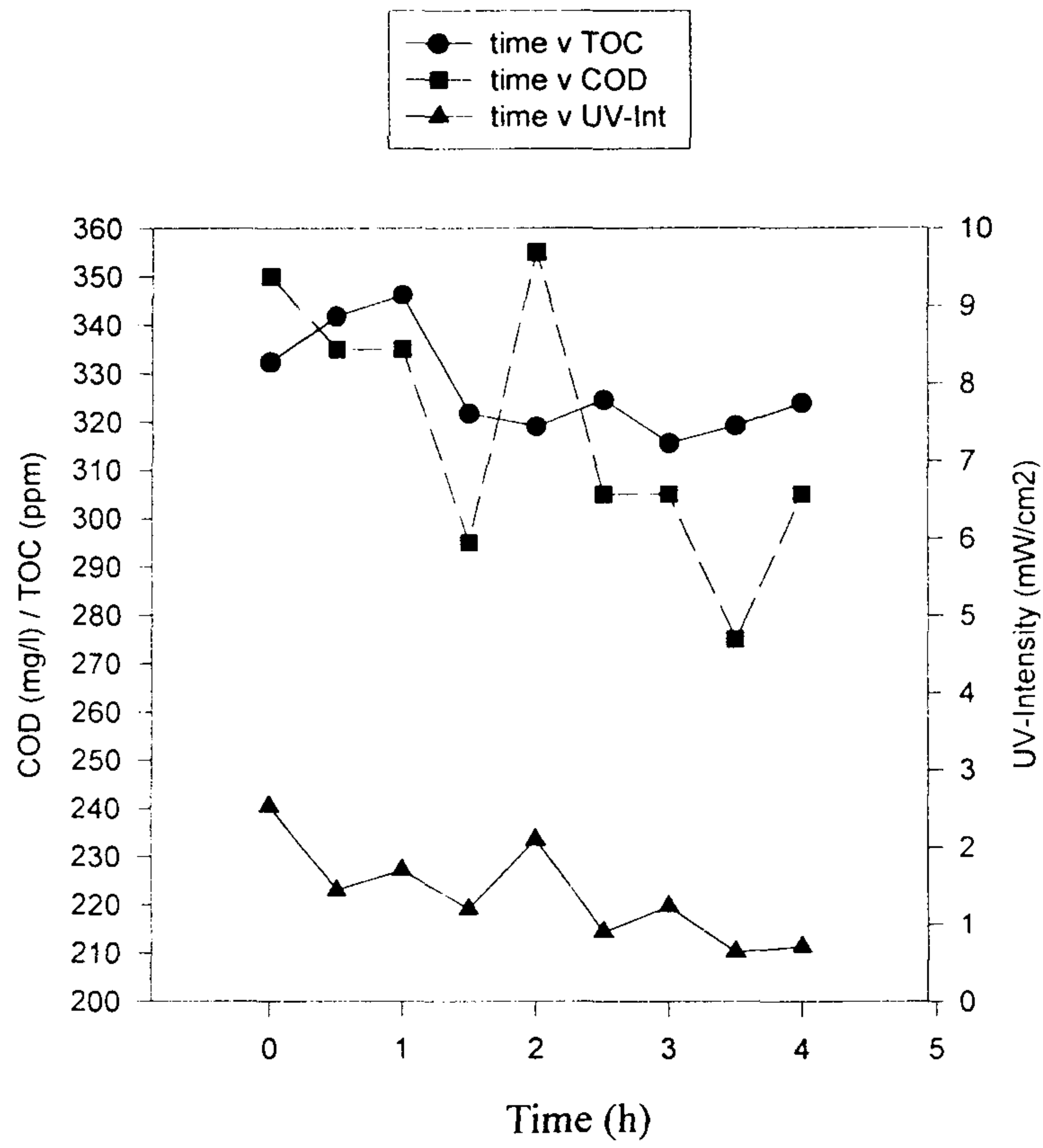


Figure 4.14 H_2O_2/ORG (1:1), 5g/l P25, pH=8.8

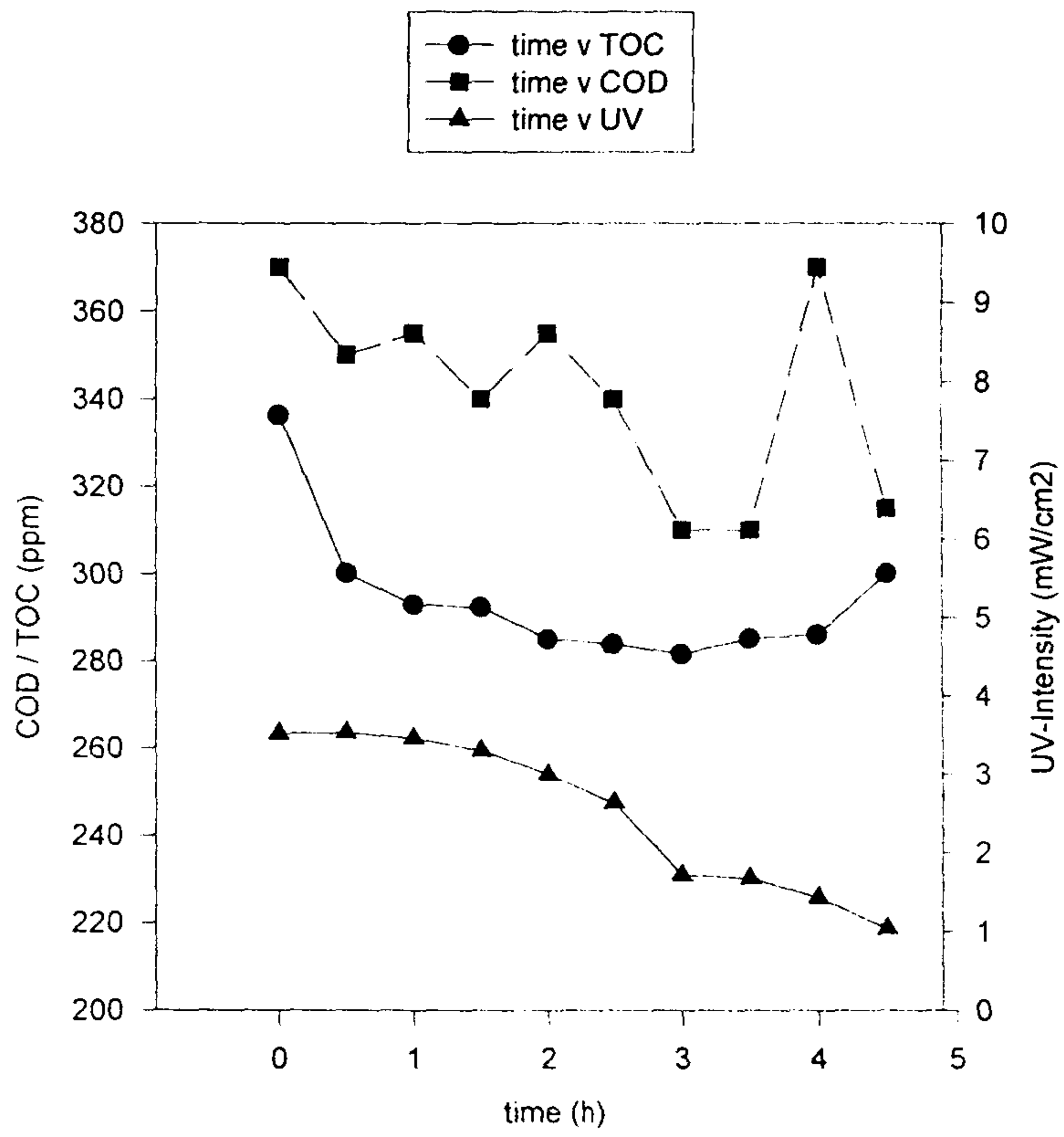


Figure 4.15 H_2O_2/ORG (1:1), 5g/l Hombikat, pH=7.6

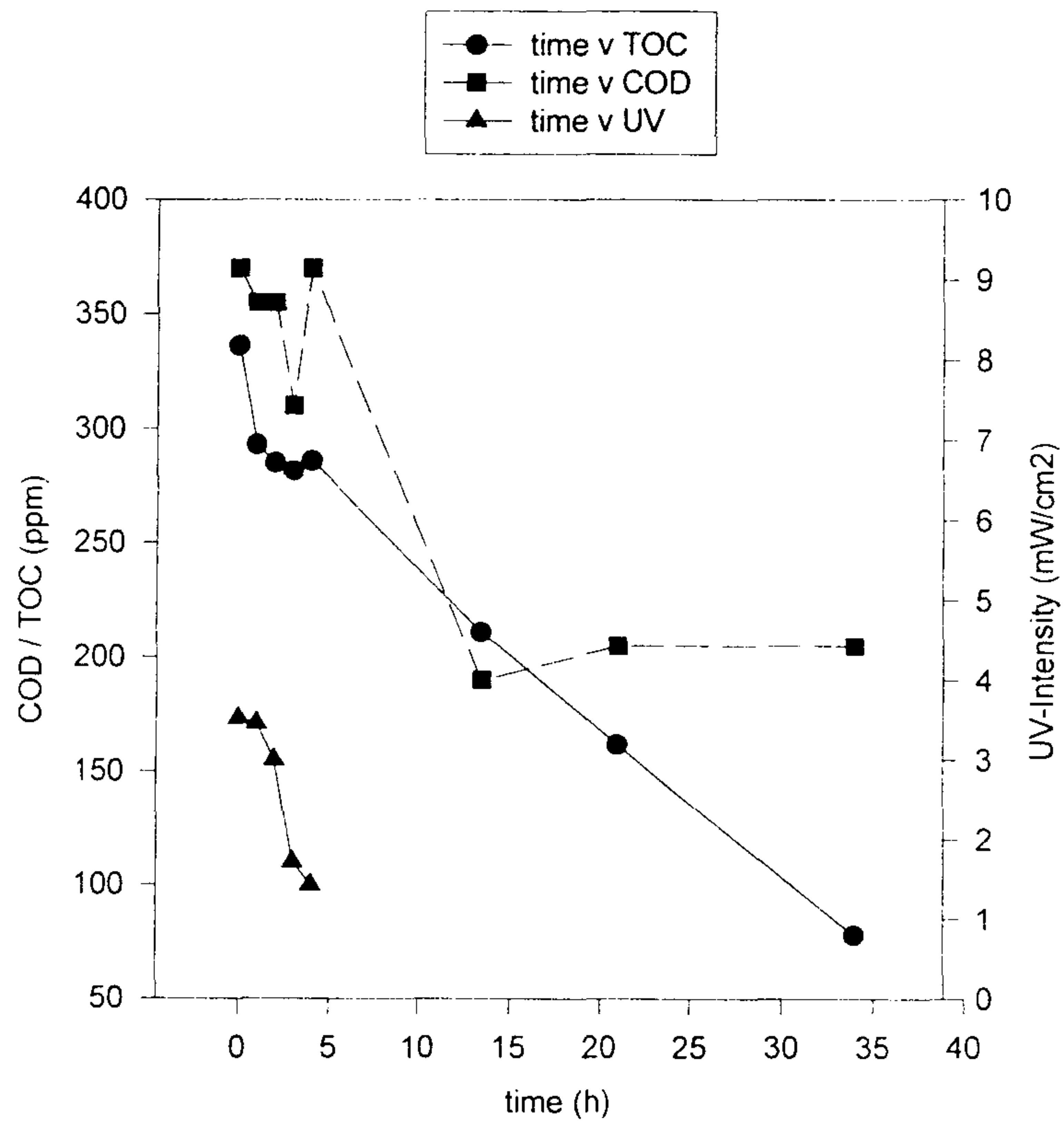


Figure 4.16 H_2O_2/ORG (1:1), 5g/l Hombikat, pH=7.6 (II)

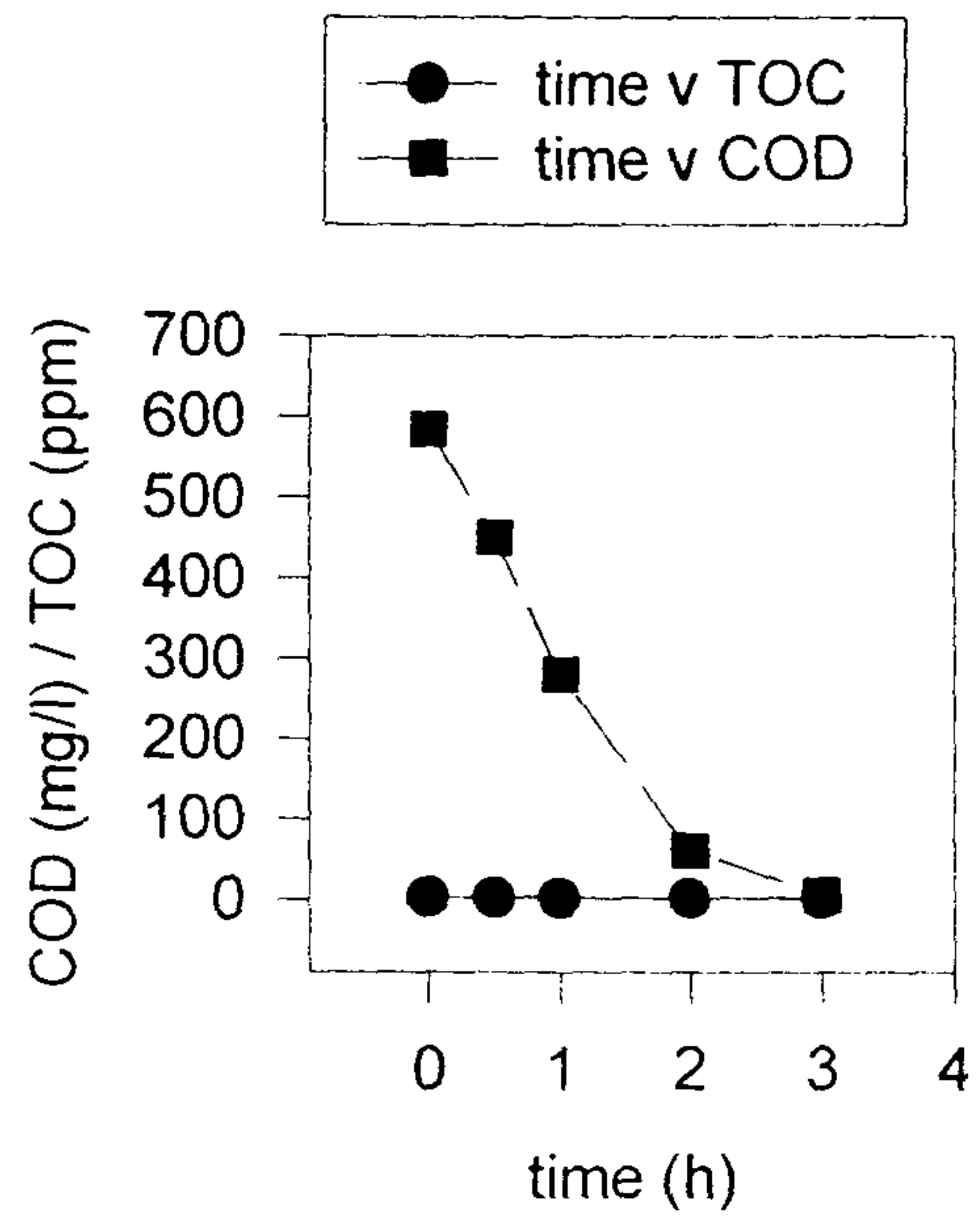


Figure 4.17 Lab experiment, H_2O_2 , 1g/l P25, pH=3, O_2 , UV-C

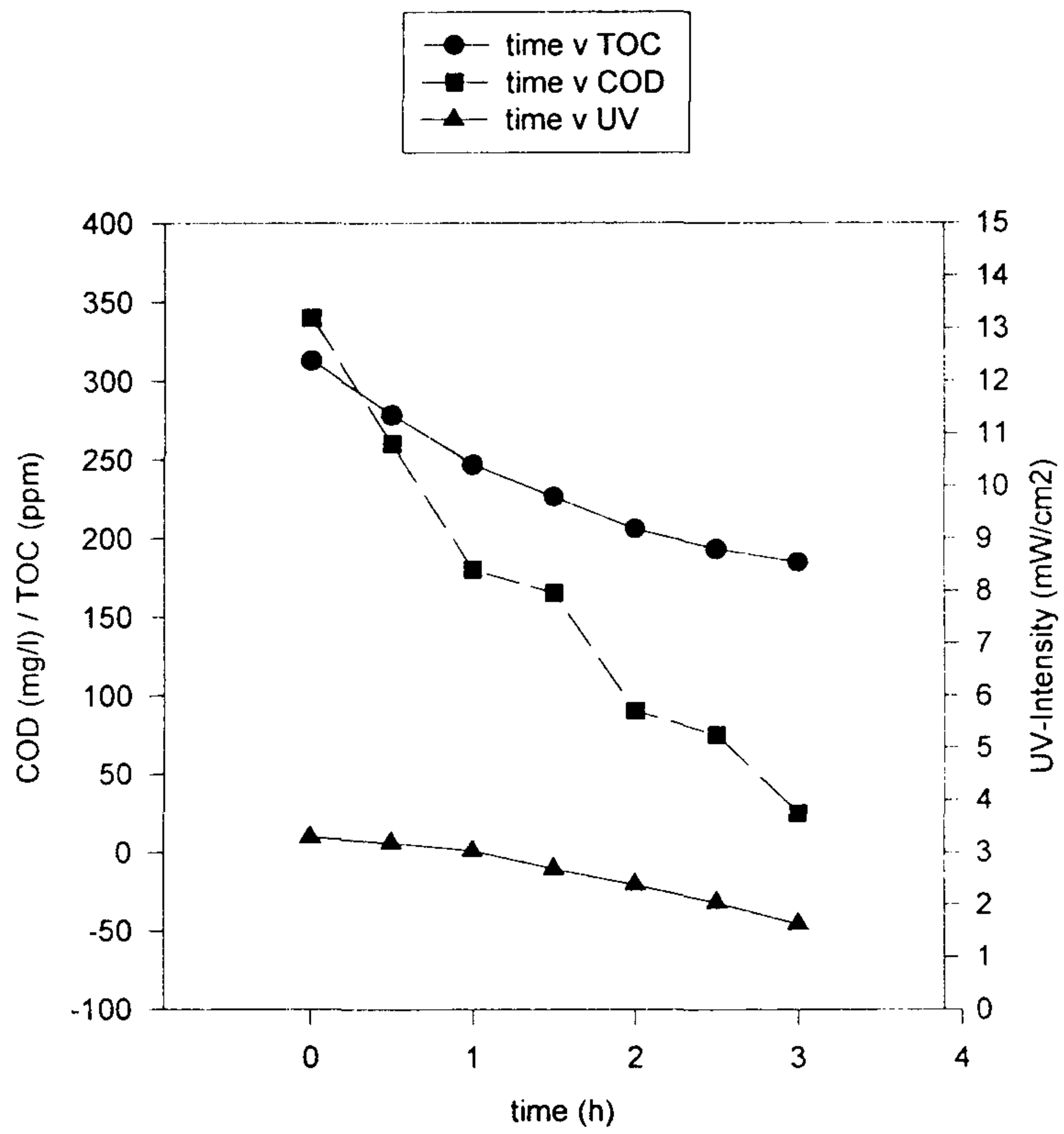


Figure 4.18 H_2O_2/ORG (1:1), 5g/l Hombikat, pH=2.9, air

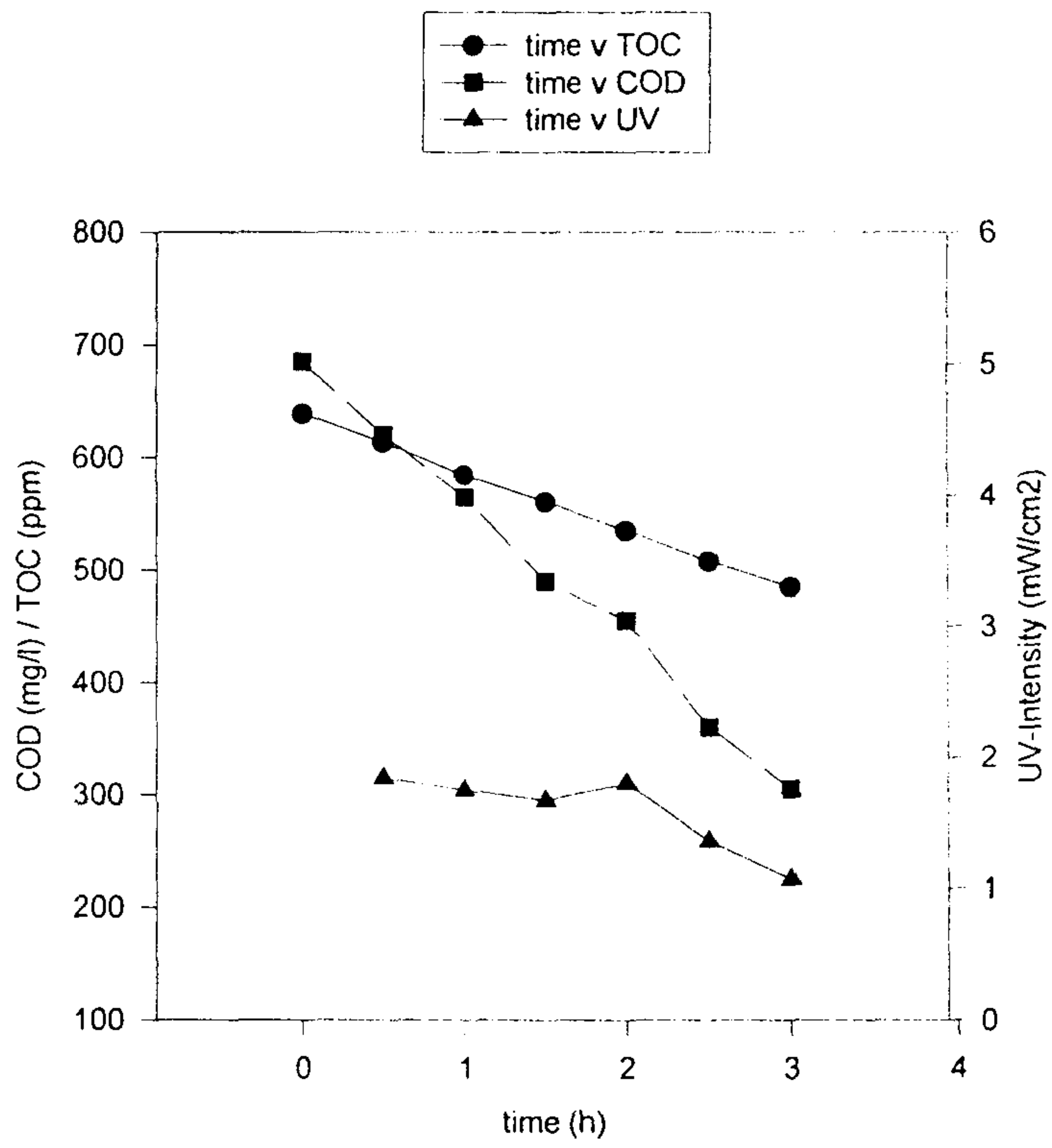


Figure 4.19 ORG, 5g/l Hombikat, pH=2.9, air

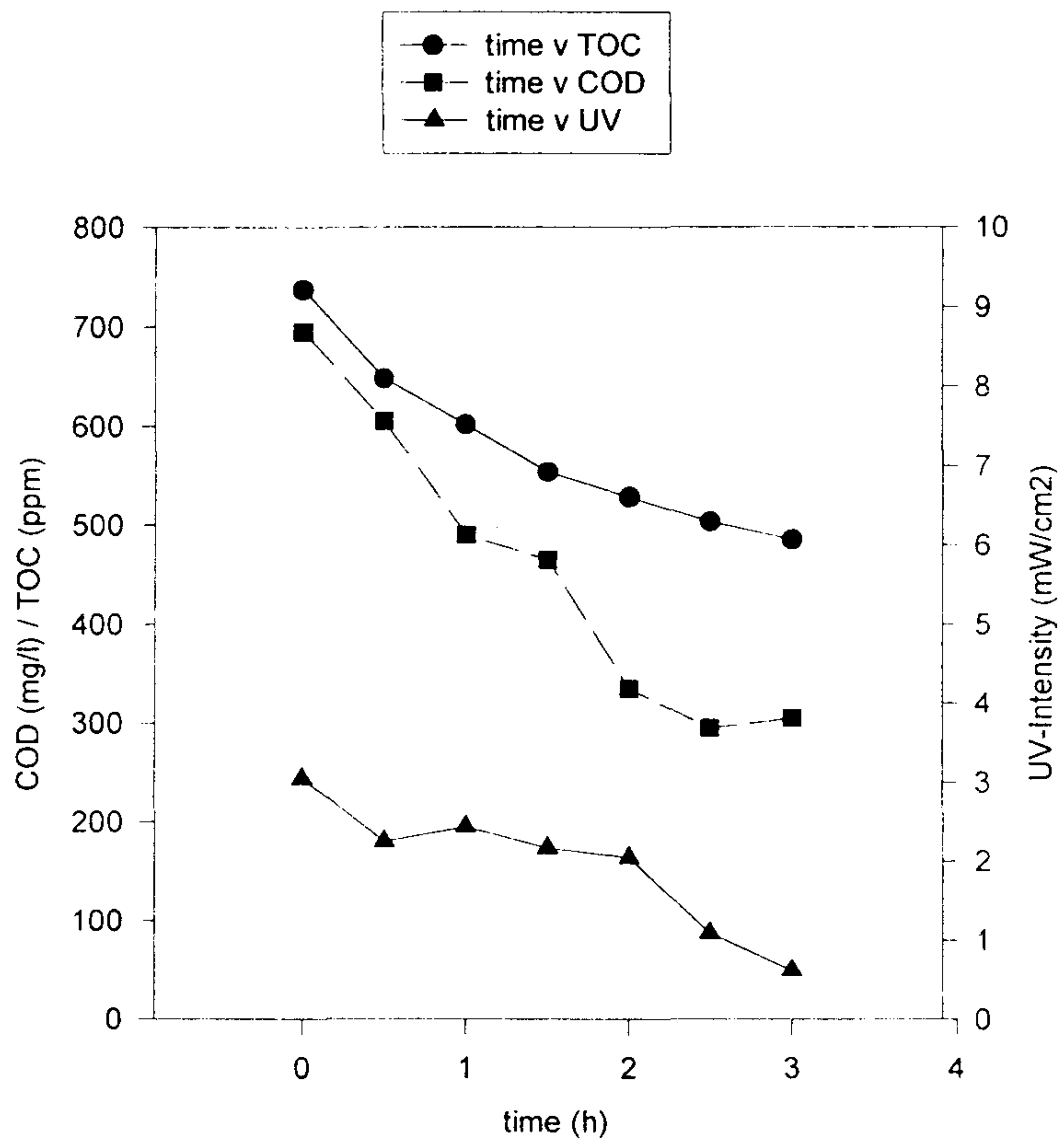


Figure 4.20 ORG, 5g/l P25, pH=2.6, air

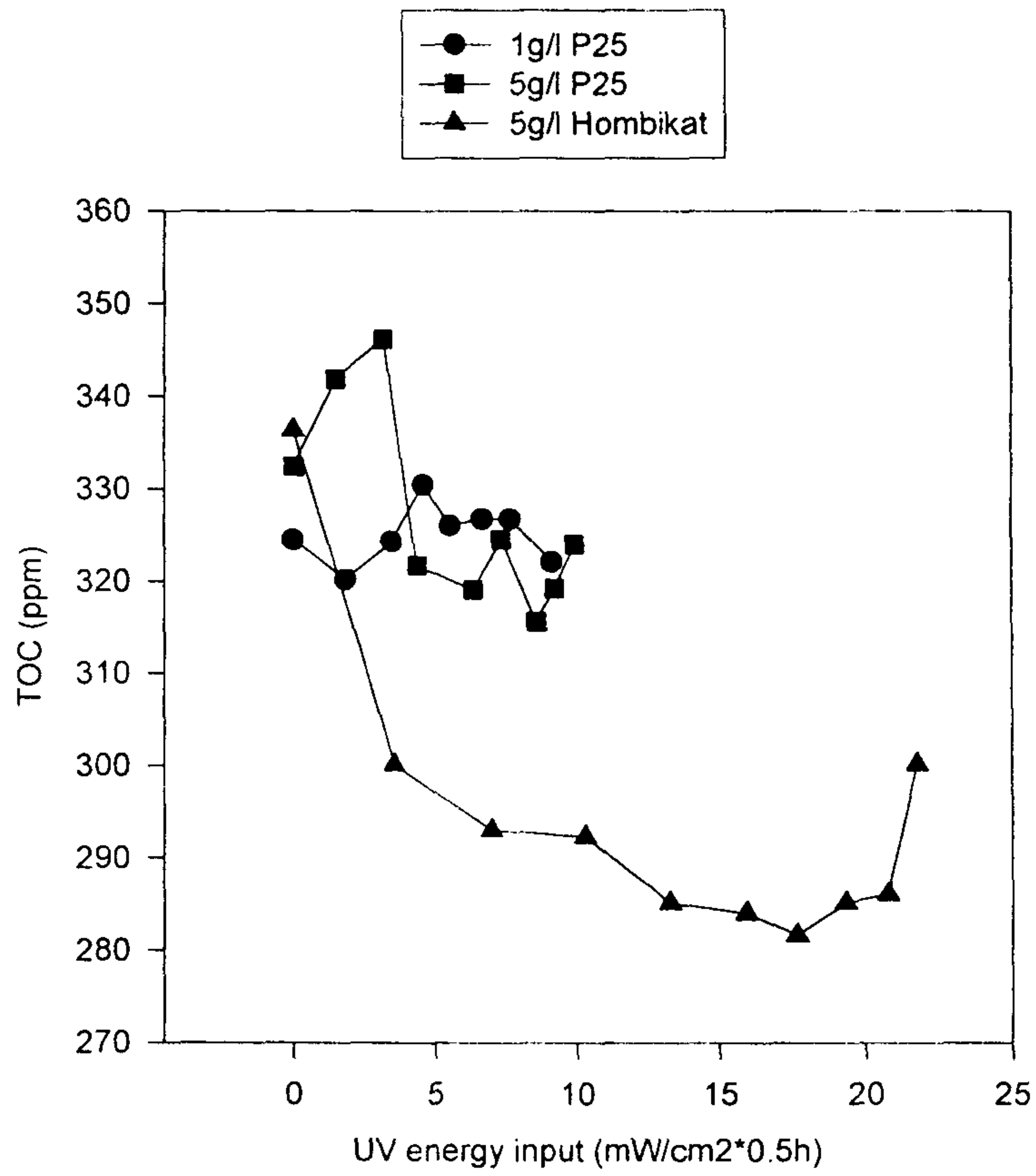


Figure 4.21 Efficiencies for H₂O₂/ORG without pH adjusting using different catalysts

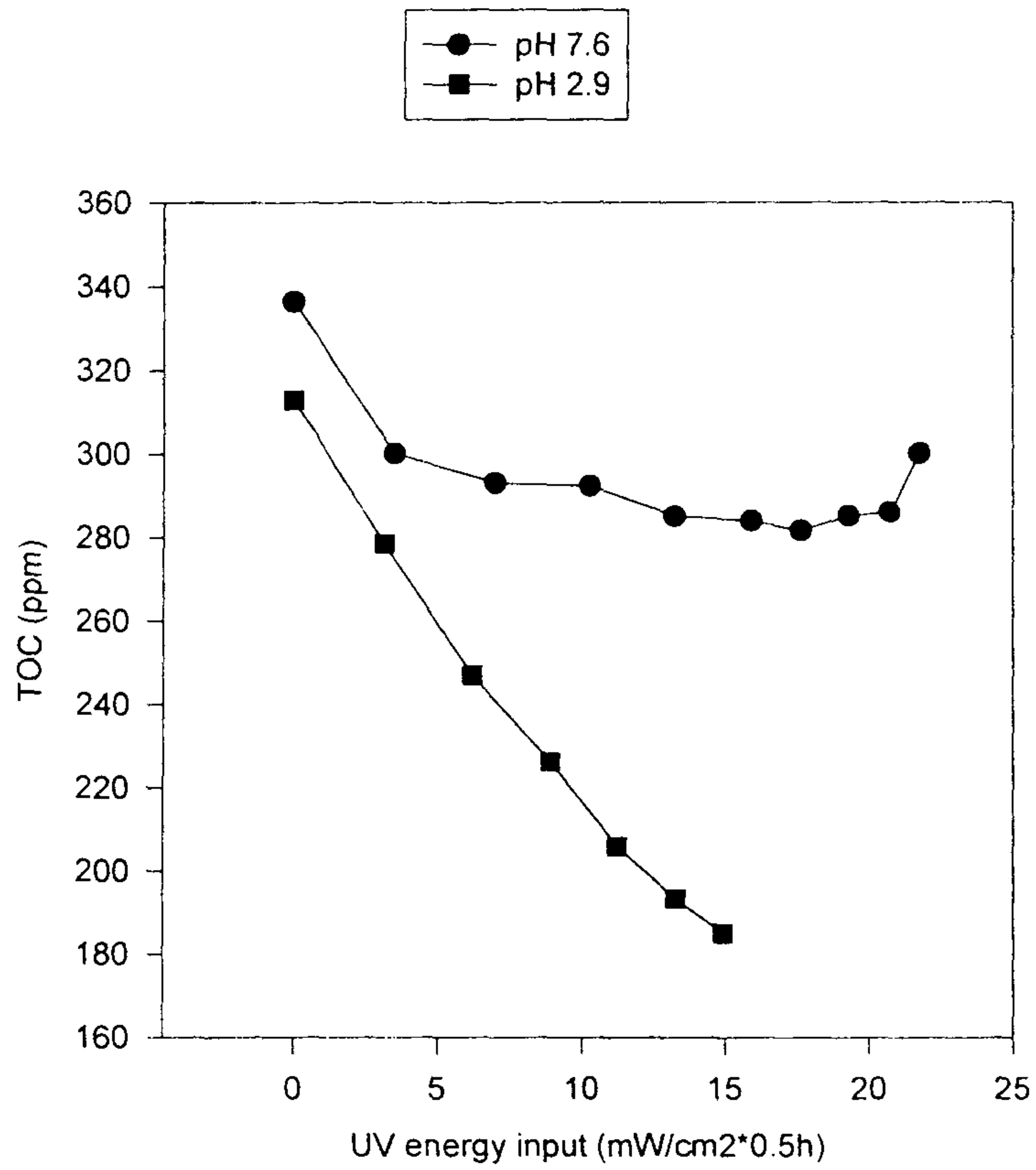


Figure 4.22 Efficiencies for H₂O₂/ORG with 5g/l Hombikat and different pH

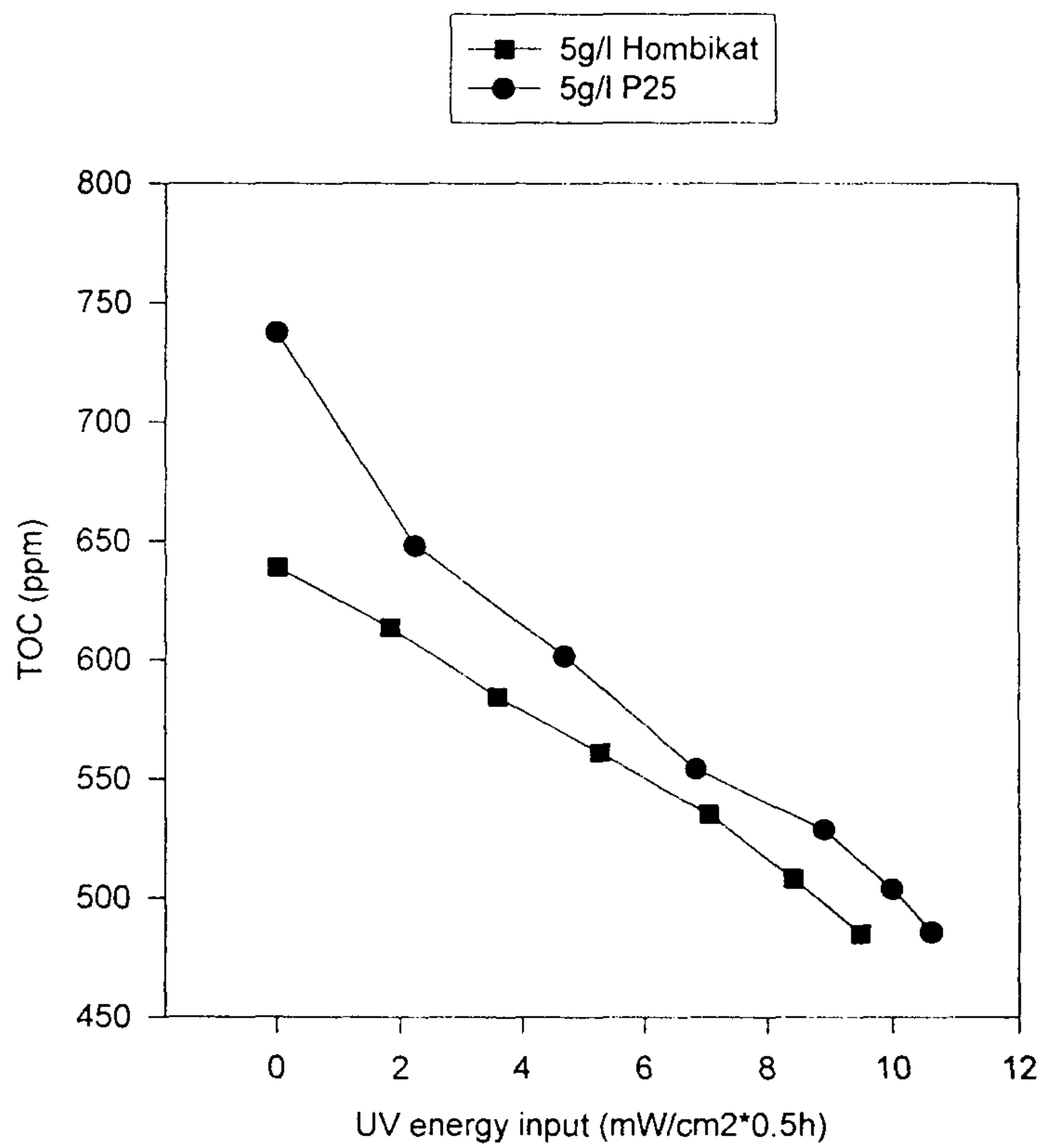


Figure 4.23 Efficiencies for ORG with pH adjusting using different catalysts

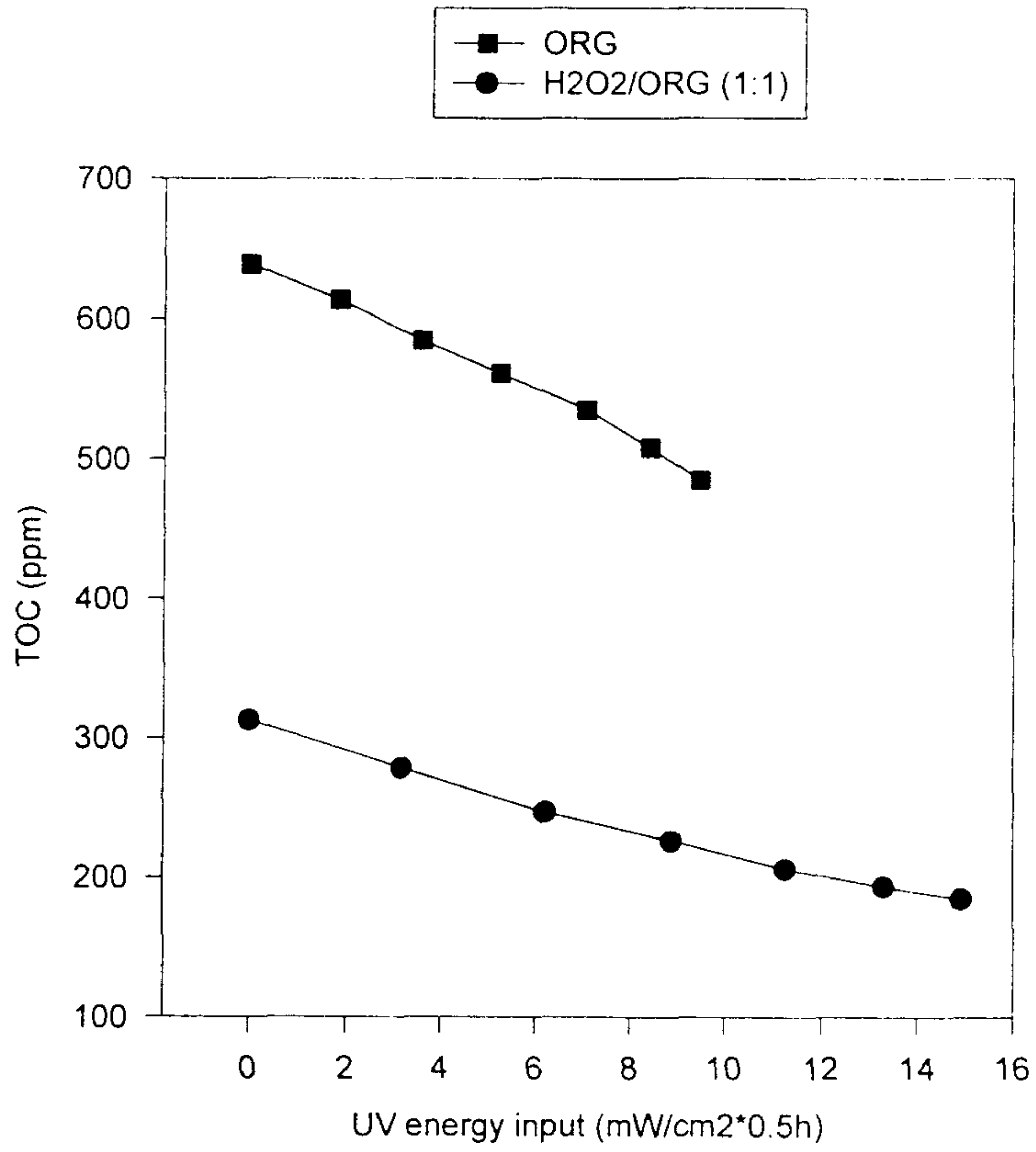


Figure 4.24 Influence of H₂O₂ on efficiency with pH adjusting using 5g/l Hombikat

4.5.4. Thoughts about scale-up calculations

The most interesting and important thing when a researcher treats real wastewater experiments is to calculate and to plan the real application system. At first one has to calculate the size of the DSSR. Presented here is a way of doing this calculation. This calculation is based on the system used in this report; one DSSR, one reservoir, one pump and one UV meter.

From the envisaged data, for complete cleaning of $V_m = 20$ liter of the wastewater with the initial TOC of X ppm UV energy input $E_m = Y \text{ mW/cm}^2 \times 0.5\text{h} \times (1.4 \times 10^4) \text{ cm}^2$ is required where $1.4 \times 10^4 \text{ cm}^2$ is equal to the area of one DSSR. Next let the amount of degraded, Q_a , to be $Z \text{ m}^3/\text{h}$ with the initial TOC, X ppm. Since the needed energy input E_a for total cleaning of Q_a is proportional to the data obtained from previous study, there is the relation

$$\frac{dE_a/dt}{Q_a} = \frac{E_m}{V_m} \Rightarrow \frac{dE_a}{dt} = Q_a \times E_m / V_m \quad (\text{A.5})$$

Additionally if we know the energy flux of solar irradiation per unit area, $dE_s/dt/m^2$, there is the equation as follows,

$$\frac{dE_a/dt}{A_a} = dE_s/dt/m^2 \quad (\text{A.6})$$

where A_a = needed area of plexiglass reactors.

Therefore,

$$A_a \left[m^2 \right] = (dE_a/dt) / (dE_s/dt) = \frac{Q_a \times E_m}{V_m \times (dE_s/dt)} \quad (\text{A.7})$$

Because all the parameters in equation (A.7) are well known the required size of reactor area can easily be determined. The primary advantage of this method described above is that there is no need to know anything about species in the wastewater and about the reaction kinetics of these compounds. Only thing we need to know is how much UV energy is needed to totally clean the water. Fortunately that is rather easy to measure.

Besides the method aforementioned there is another method for doing this calculation. This method tries to calculate photonic efficiencies for the photocatalytic degradation. But in this calculation the amount of substances degraded than just TOC is requested. As a result, the second method will be preferred in the case of wastewater which contains small number of compounds.

Chapter 5. Conclusions

A) Among the prepared three different mixed oxides, Fe/Ti, Ni/Ti, and Zn/Ti, Fe/Ti showed red-shifted absorbance trends, resulting in higher photonic efficiency than pure TiO₂ and the other mixed oxides. In addition, characteristic peak of H₂O at 3250 cm⁻¹ revealed that only Fe/Ti had the increased area under that peak as the content of impurity (Fe) increased.

B) For an efficient treatment of the waste waters pH adjusting is the most important parameter because this fastens the degradation rate about 5 times.

C) In two different comparisons P25 was about 1.4 times more efficient than Hombikat. So P25 can be recommended for the treatment of these waste waters. As catalyst concentration 5g/l seems to be more efficient than 1g/l.

D) The influence of H₂O₂ on the degradation process can not clearly be deduced from the measured data. It is just known that the influence is in the range of 1.3 times faster to 0.6 times slower.

References

1. Hoffmann, M. R., Martin, S. T., Choi, W., and Bahnemann, D. W., *Chem. Rev.* **95**, 69 (1995).
2. Jordan, P. H., and Yue, P. L., in "Photocatalytic Purification and Treatment of Water and Air." (D. F. Ollis and H. Al-Ekabi, Eds.) Elsevier Science Publishers, New York, 1993.
3. Bahnemann, D. W., Cunningham, J., Fox, M. A., Pelizzetti, E., Pichat, P., and Serpone, N., "Aquatic and Surface Photochemistry." (G. R. Helz, R. G. Zepp, and D. G. Crosby, Eds.) Lewis Publishers, Boca Raton, 1994.
4. Moser, J., Gratzel, M., and Gallay, R., *Helv. Chim. Acta*, **70**, 1596, (1987)
5. Bahnemann, D. W., Bockelmann, D., Goslich, R., and Hilgendorff, M., in Proceedings of ENERGEX '93, Seoul, Korea, October 1993.
6. Nozik, A. J., in "Photocatalytic Purification and Treatment of Water and Air." (D. F. Ollis and H. Al-Ekabi, Eds.) Elsevier Science Publishers, New York, 1993.
7. Bockelmann, D., Lindner, M., and Bahnemann, D. W., in "Fine Particles Science and Technology" (E. Pelizzetti, Eds.) Kluwer Academic Publishers, Netherlands, 1996.
8. Memming, R., *Topics Curr. Chem.*, 143, 79 (1988)
9. Bahnemann, D. W., *Israel Journal of Chemistry*, 33, 115 (1993).
10. Overheim R. D. and Wagner, D. L., *Light and Color*, 1982.

11. Hilgendorff, M., Bockelmann, D., Nogueira, R. F. P., Weichgrebe, D., Jardim, W. F., Bahnemann, D., and Goslich, R., in Proceedings of 6th International Symposium on Solar Thermal Concentrating Technologies, Vol 2, 1167 (1992).
12. Bahnemann, D. W., Hilgendorff, M., and Memming, R., *J. Phys. Chem. B.*, 101, 4265 (1997).
13. Turchi, C. S. and Ollis, D. F., *J. Catal.*, 122, 178 (1990).
14. Bahnemann, D. W., EPA Newsletter, 48, 59 (1993).
15. Dillert, R., and Bahnemann, D. W., EPA Newsletter, 52, 33 (1994).
16. Lindner, M., Bahnemann, D. W., Hirthe, B., and Griebler, W., in “Solar Engineering”, (W. B. Stine, T. Tanaka, and D. E. Claridge Eds.), The American Society of Mechanical Engineers, 399 (1995).
17. Kormann, C., Bahnemann, D. W., and Hoffmann, M. R. *J. Photochemistry and Photobiology A: Chemistry*, 48, 161 – 169 (1989).
18. Müller, B. R., Majoni, S., Memming, R., and Meissner, D., *J. Phys. Chem. B.*, 101 (14), 2501 (1997).
19. Kormann, C., Bahnemann, D. W., and Hoffmann, M. R., *J. Phys. Chem. B.*, 92, 5196 (1988).
20. Turchi, C. S. and Ollis, D. F., *J. Phys. Chem.*, 92, 6852 (1988).

여 백

APPENDIX

Photographs of a couple of photoreactors and prepared mixed oxides

여 백



Figure A. 1 One sun flat plate photoreactor



Figure A.2 Bench scale photoreacot with UV light

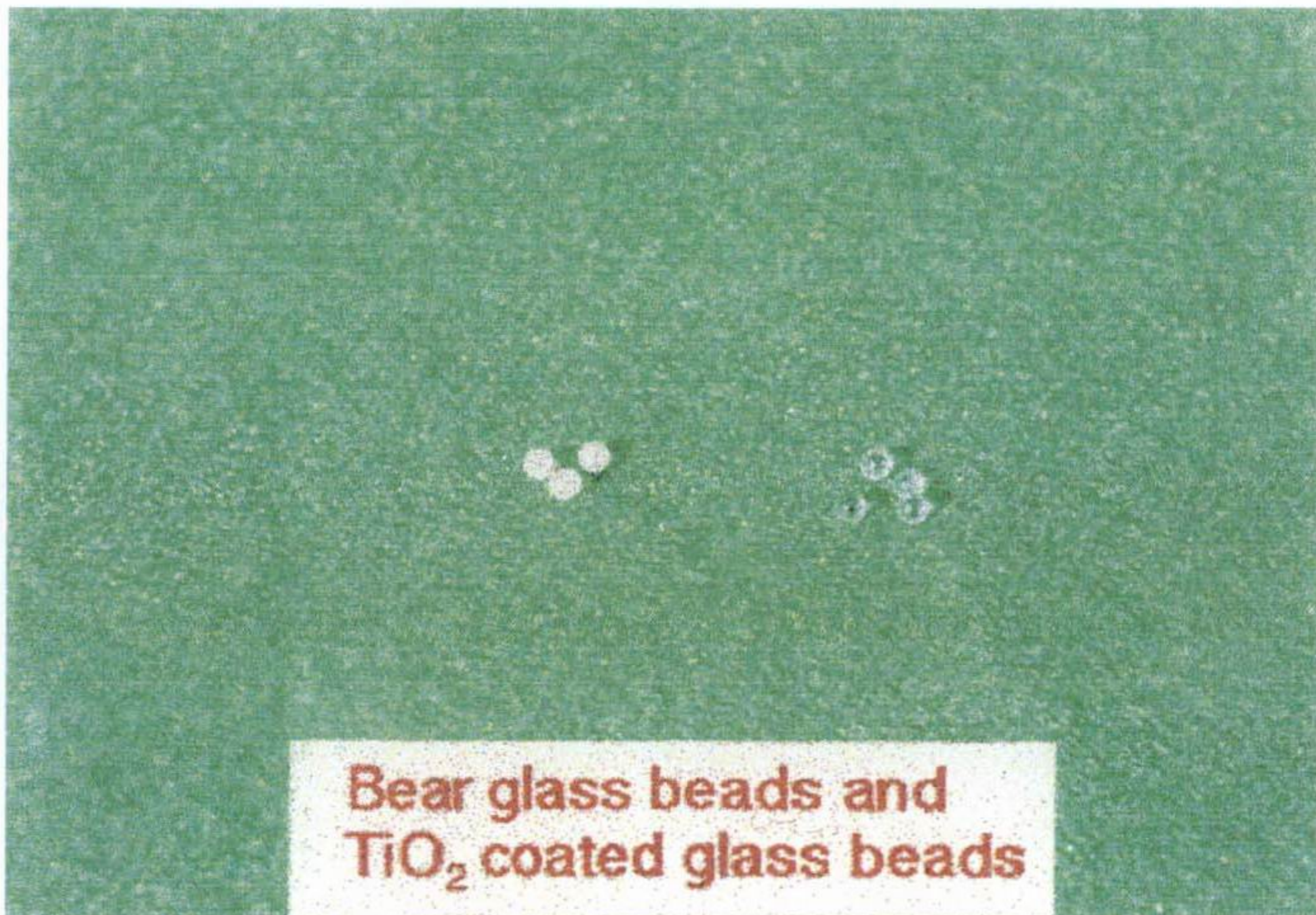


Figure A.3 Coated titanium dioxide for future application

여 백

Principle of Photochemical Reactor

여 백

Because the research on the utilization and application of photochemical reactor for homogeneous system has been conducted by many researchers, the theoretical background of modeling and scaling up is established. However, it has not been long to study the heterogeneous system. Hence, basic classification design method are follows.

A.1 Type of photoreactor

(1) by operation type

- batch; for slow reaction rate
- semi-batch and recirculation
- continuous (CSTR, PFR); for fast reaction rate

Since the reaction rate is the function of reaction mechanism, catalyst, temperature, pressure, and initial concentration, the decision on the type of reactor is flexible.

(2) by phase

- Single phase; for gas and liquid
- Multi-phase; gas and liquid, gas and solid, liquid and solid, and gas, liquid, solid.

If gas is included in reactants, continuous type is recommended due to increasing volume. Besides depending the rate of decay of catalyst type selection is required.

(3) by thermal transfer

- Batch type is designed for easy heat apply and removal, but continuous might need extra facility. The heat effects to be considered are increase in temperature by absorption of photon and reaction rate.

(4) by flow and mixing characteristics

- Completely mixed
- Some back mixing
- Plug flow
- Nonideal flow characteristics

(5) by applied catalysts

- Slurry type
- Thin film
- Packed bed
- Fluidized bed

So far, slurry type using powdery catalyst has been proven most efficiency, but it has separation problem at the end. However, the others do not have the separation problem, but lower efficiency than slurry type.

Generally speaking, rate-governing factors are selected by flow and mixing

characteristics, and contact of catalyst with reactants. For this reason, the design of optimum residence time and contact time is essential. In addition, back mixing should not be excluded as well as diffusion process. More importantly, the mutual relation between reaction parameters must be investigated.

The material of reactor must be selected by temperature, pressure, and corrosion factor of reactants, products, and heat transfer media. Commonly it is made out of optical glass, pyrex glass, vycor glass, quartz or plexiglass. Even though quartz has excellent light transmit ability, it costs too much and is not easily made. For shorter wavelength than 300 nm quartz is the only selection. Investigating the absorbance of UV-VIS between 190 and 300 nm reactor material can be chosen.

A.2 Modeling of photoreactor

For the purpose of photoreactor analysis of physical and chemical process is required. On the basis that mass balance and thermodynamic data are known, relation between those mentioned below need to be dissolved.

- Concentration of reactants
- Reaction conversion yield
- Selectivity
- Reactor size and amount of catalyst
- Heat transfer rate

1. Mass conservation for component j

$$\text{Rate}_{\text{accumulation},j} = \text{Rate}_{\text{into reactor}, m_j} - \text{Rate}_{\text{out of reactor}, m_j} + \text{Rate}_{\text{change}, m_j} \quad (\text{A.1})$$

: m_j = mass of jth species

2. Momentum

$$\text{Rate}_{\text{accumulation}, \Delta \text{momentum}} = \text{Rate}_{\text{inlet reactor}, \Delta \text{momentum}} - \text{Rate}_{\text{outlet of reactor}, \Delta \text{momentum}} + \text{Rate}_{\text{change}, \Delta \text{momentum}} \quad (\text{A.2})$$

: Δ momentum = momentum change.

3. Energy

$$\text{Rate}_{\text{accumulation}, \text{energy}} = \text{Rate}_{\text{inlet reactor}, \text{energy}} - \text{Rate}_{\text{outlet reactor}, \text{energy}} + \text{Rate}_{\text{change}, \text{energy}} \quad (\text{A.3})$$

4. Radiation

$$\text{Spatial distribution}_{I, \text{radiant energy}} + \text{Volumetric Rate}_{\text{Ads}, \text{radiant energy}} = 0 \quad (\text{A.4})$$

To solve these differential equations boundary conditions needs to be known, The final term at the right side of eq. (A.1) represents reaction equation, and affected by eq (A.4). Hence, solution of eq (A.1) shows the concentration distribution.. Distribution of rate and temperature can be obtained from the solutions of eq (A.2) and (A.3). Eq (A.2) affects eq (A.1) and (A.3). These

equations are connected with each other like mentioned above, usually numerical tool must be applied, not analytical analysis. Aforementioned equations can be trimmed using theoretically reasonable assumptions.. If ideal case can be assumed, accumulation term can be eliminated. In the case of batch system, inout and output term can be eliminated. In addition, momentum equation is not nessary for the case of completely mixing.

Equation (A.4) needs to be considered in terms of factors described below.

- Type of reactor
- Thickness
- Position of light source
- wavelength
- Mixing characteristics
- Home- or hetero-geneous media